

South Dakota State University

Open PRAIRIE: Open Public Research Access Institutional Repository and Information Exchange

Electronic Theses and Dissertations

2020

Particle Injection Simulation on Cold Spray Technology

Christopher A. Santini

South Dakota State University

Follow this and additional works at: <https://openprairie.sdstate.edu/etd>



Part of the [Mechanical Engineering Commons](#), and the [Physics Commons](#)

Recommended Citation

Santini, Christopher A., "Particle Injection Simulation on Cold Spray Technology" (2020). *Electronic Theses and Dissertations*. 4991.

<https://openprairie.sdstate.edu/etd/4991>

This Thesis - Open Access is brought to you for free and open access by Open PRAIRIE: Open Public Research Access Institutional Repository and Information Exchange. It has been accepted for inclusion in Electronic Theses and Dissertations by an authorized administrator of Open PRAIRIE: Open Public Research Access Institutional Repository and Information Exchange. For more information, please contact michael.biondo@sdstate.edu.

PARTICLE INJECTION SIMULATION ON COLD SPRAY TECHNOLOGY

BY:

CHRISTOPHER A. SANTINI

A thesis submitted in partial fulfillment of the requirements of the

Master of Science

Major in Mechanical Engineering

South Dakota State University

2020

THESIS ACCEPTANCE PAGE

Christopher Alexis Santini

This thesis is approved as a creditable and independent investigation by a candidate for the master's degree and is acceptable for meeting the thesis requirements for this degree.

Acceptance of this does not imply that the conclusions reached by the candidate are necessarily the conclusions of the major department.

Jeffrey Doom
Advisor

Date

Kurt Bassett
Department Head

Date

Nicole Lounsbery, PhD
Director, Graduate School

Date

ACKNOWLEDGEMENTS

I would like to specially thank my advisor Dr. Jeffrey Doom for all his support and advising help. He has been my inspiration to continue my Masters in the field of CFD research and has taught me so much, I'm eternally grateful. I would also like to acknowledge the support of the faculty of the Department of Mechanical Engineering for giving me such wonderful education and place to work at South Dakota State University.

A special thank you to my parents William Santini and Lucienne Gascot for always being supportive of my dreams to become an engineer. They have helped me in emotional and economic support through my entire college career. Also would like to thank all my friends and class mates that have supported me throughout all my schooling, a special thank you to Marcela Salas for the unconditional support.

The Surface Engineering Research Collaboration grant supports this work through the Graduate Research Assistantship. Computing resources were provided by University Networking and Research Computing and Department of Mechanical Engineering at South Dakota State University. Simulation parameters were provided by AMP Laboratory, South Dakota School of Mines and Technology.

TABLE OF CONTENTS

NOMENCLATURE	vi
LIST OF FIGURES	viii
LIST OF TABLES	xii
ABSTRACT	xiii
CHAPTER 1: INTRODUCTION	1
History	2
Working Principle	4
Cold Spray Systems	6
Cold Sprayed Coatings	9
Applications of cold spray technology	10
Essential Parameters to be controlled in Cold Spray	13
Modeling and simulation of Cold Spray	14
CHAPTER 2: LITERATURE REVIEW	15
Research Objective	21
CHAPTER 3: METHOD AND APPROACH	22
Problem statement	23

Geometry	24
CAD Model Generation	26
Discretization.....	26
Physics.....	29
Solver Settings	33
CHAPTER 4: RESULTS AND DISCUSSION.....	35
Simulation procedure in Starccm+	36
Visualization	44
Summary of the Results	62
Validation	64
Research Contribution.....	67
CHAPTER 5: CONCLUSION AND FUTURE WORK	68
REFERENCES	69

NOMENCLATURE

V_0 : Inlet velocity of the carrier gas, m/s

P_0 : Inlet Pressure of the carrier gas, pa

T_0 : Inlet Temperature of the carrier gas, °C

ρ_0 : Density at Inlet of the carrier gas, kg/m³

c_p : Specific heat at constant-pressure, J/kg K

c_v : Specific heat constant-volume, J/kg K

V^* : Carrier gas velocity at nozzle throat, m/s

P^* : Carrier gas pressure at nozzle throat, pa

T^* : Carrier gas temperature at nozzle throat, °C

ρ^* : Density of the carrier gas at the nozzle throat, kg/m³

A^* : Cross-sectional area at the nozzle throat, m²

R : Gas constant, J/mol·K (8.314 J/mol·K)

\dot{m} : Mass flow rate, kg/s

M : Mach number

γ : Adiabatic Index

m_p : DEM particle of mass

F_d : Drag force

F_p : Pressure gradient force

F_{vm} : Virtual mass force

F_g : Gravity force

F_u : user-defined body force

F_c : Contact force

F_{Co} : Coulomb force

ρ : density.

$\bar{\mathbf{V}}$: mean velocity.

\bar{P} : mean pressure.

\mathbf{I} : identity tensor.

$\bar{\mathbf{T}}$: mean viscous stress tensor.

\mathbf{f}_b : resultant of the body forces (such as gravity and centrifugal forces).

\bar{E} : mean total energy per unit mass.

$\bar{\mathbf{q}}$: mean heat flux.

ϕ : represents velocity components, pressure, energy or species concentration

$\bar{\phi}$: mean or average value

ϕ' : Fluctuating component

LIST OF FIGURES

Figure 1: Schematic of Thurston's design [2]	2
Figure 2: Early Russian Tunnel Experiments (a) Copper particles at 250m/s: Erosion (b) Copper particles at 900m/s: Deposition [4]	3
Figure 3: The First device for applying a coating by cold spray patented in 1986 [4]	4
Figure 4: Cold spray system component example	5
Figure 5: Particle temperature and velocity map [7].....	6
Figure 6: Low-Pressure Cold Spray system [6]	7
Figure 7: High-Pressure Cold Spray system [6]	8
Figure 8: Step Drilled Nozzle Geometry.....	24
Figure 9: Step Drilled Nozzle CAD Model	26
Figure 10: Step Drilled Nozzle Mesh.....	28
Figure 11: Model Showing Boundary Conditions	34
Figure 12: Visualization of Velocity Magnitude in Step Drilled Nozzle	44
Figure 13: Visualization of Absolute Pressure in Step Drilled Nozzle	44
Figure 14: Visualization of 500 particles per second in Step Drilled Nozzle.....	45
Figure 15: Visualization of residual plot for Step Drilled Nozzle	45

Figure 16: Visualization of Velocity Magnitude in Step Drilled Nozzle	46
Figure 17: Visualization of Absolute Pressure in Step Drilled Nozzle	46
Figure 18: Visualization of 1000 particles per second in Step Drilled Nozzle	47
Figure 19: Visualization of residual plot for Step Drilled Nozzle	47
Figure 20: Visualization of Velocity Magnitude in Step Drilled Nozzle	48
Figure 21: Visualization of Absolute Pressure in Step Drilled Nozzle	48
Figure 22: Visualization of 2000 particles per second in Step Drilled Nozzle	49
Figure 23: Visualization of residual plot for Step Drilled Nozzle	49
Figure 24: Visualization of Velocity Magnitude in Step Drilled Nozzle with Nitrogen.....	50
Figure 25: Visualization of Absolute Pressure in Step Drilled Nozzle with Nitrogen.....	50
Figure 26: Visualization of 2000 particles per second in Step Drilled Nozzle with Nitrogen	51
Figure 27: Visualization of residual plot for Step Drilled Nozzle with Nitrogen	51
Figure 28: Visualization of Velocity Magnitude in Step Drilled Nozzle with Nitrogen.....	52
Figure 29: Visualization of Absolute Pressure in Step Drilled Nozzle with Nitrogen.....	52
Figure 30: Visualization of 1000 particles per second in Step Drilled Nozzle with Nitrogen	53
Figure 31: Visualization of residual plot for Step Drilled Nozzle with Nitrogen	53
Figure 32: Visualization of Velocity Magnitude in Step Drilled Nozzle with Nitrogen.....	54

Figure 33: Visualization of Absolute Pressure in Step Drilled Nozzle with Nitrogen.....	54
Figure 34: Visualization of 500 particles per second in Step Drilled Nozzle with Nitrogen	55
Figure 35: Visualization of residual plot for Step Drilled Nozzle with Nitrogen	55
Figure 36: Visualization of Velocity Magnitude in Step Drilled Nozzle with Helium.....	56
Figure 37: Visualization of Absolute Pressure in Step Drilled Nozzle with Helium.....	56
Figure 38: Visualization of 2000 particles per second in Step Drilled Nozzle with Helium.....	57
Figure 39: Visualization of residual plot for Step Drilled Nozzle with Helium	57
Figure 40: Visualization of Velocity Magnitude in Step Drilled Nozzle with Helium	58
Figure 41: Visualization of Absolute Pressure in Step Drilled Nozzle with Helium.....	58
Figure 42: Visualization of 1000 particles per second in Step Drilled Nozzle with Helium.....	59
Figure 43: Visualization of residual plot for Step Drilled Nozzle with Helium	59
Figure 44: Visualization of Velocity Magnitude in Step Drilled Nozzle with Helium	60
Figure 45: Visualization of Absolute Pressure in Step Drilled Nozzle with Helium.....	60
Figure 46: Visualization of 500 particles per second in Step Drilled Nozzle with Helium	61
Figure 47: Visualization of residual plot for Step Drilled Nozzle with Helium	61
Figure 48: Calculated Velocity profile concerning the nozzle axis for cold spray supersonic jet at 800 C and 3 MPa [Validation Case]	65

Figure 49: Computed velocity profile in the nozzle axis for cold spray supersonic nozzle jet 250 C	
and 3.2 MPa [current study]	66

LIST OF TABLES

Table 1: Step Drilled Nozzle Step Dimensions	24
Table 2: Summary of Nozzle Dimensions.....	25
Table 3: Summary of Boundary Conditions used for the Nozzle	34
Table 4: Summary of Process Variables used in validation case and current case	65

ABSTRACT

PARTICLE INJECTION SIMULATION ON COLD SPRAY TECHNOLOGY

CHRISTOPHER A. SANTINI

2020

Computational Fluid Dynamics (CFD) is a useful tool when it comes to research in the fields of Aerodynamics, Turbomachinery, and is used in several other fields of research. CFD is an important tool in the engineering industry because it allows for understanding and evaluation of a new design, this can lead to advancements in developing a more efficient and effective design. This tool helps in the understanding of the flow phenomena and how it can interact with its surroundings. One of the main reasons in the use of CFD is to reduce the cost of testing a design by running simulations, whereas creating an experimental apparatus to test a design would lead to a higher cost.

A CFD analysis can be done on coating technologies to evaluate their performance and behavior. Coating technology has a wide variety of applications such as: oxidation protection, corrosion protection, aid in repairs, and thermal protection. One of the most researched coating technologies is Cold Spray Technology, this technology is relatively new and has many unique characteristics. Cold spray is used to manufacture coatings in the solid state, fully preserving the feedstock material properties. This coating is done by the compression of the carrier gas in a converging section of the nozzle, followed by a diverging section where the thermal energy is converted into kinetic energy, thereby speeding up the particles to their desired velocity and creates a non-thermal coating on the substrate.

This thesis is focused on the proper procedure that must be taken to create and run a simulation on the injection of particles into a cold spray nozzle. This procedure is broken down into the study of physics models, the desired mesh that must be analyzed and evaluated to obtain adequate simulations and results. These simulations will be able to demonstrate the behavior of the particles as they travel through the cold spray nozzle, thus being able to compare different carrier gases and evaluate which would perform better with the particles.

The studies performed were done by using different meshing densities using the k-Omega turbulent models provided in StarCCM+ solver. Validation is very important to ensure that the results are adequate. The validation step was done by comparing the simulations ran to the simulations done by Muhammad Faizan Ur Rab. By comparing the simulations we are able to validate the studies.

CHAPTER 1: INTRODUCTION

The cold spray process starts with the material particles being accelerated at very high velocity that leads to the bonding of the particles to the substrate. In this process, small powdered particles in a range of 5 to 100 μm are accelerated to a high velocity in the range of 300 to 1200 m/s in a supersonic jet of heated gas and then impinged onto a substrate surface in solid state without significant fusion, undergoing intensive plastic deformation. Cold spray produces coatings based on a wide selection of materials with superior characteristics. Before cold spray technology, it was necessary to either dissolve the metal in a chemical bath, melt them or vaporize them. Now, through cold spray technology, metals can be deposited rapidly in the solid state, and thus, drawbacks connected with melting, such as oxidation and undesirable phase transformations can be avoided.

Cold spraying is recognized as a promising spray coating technique capable of producing thick metal and in some cases metal-ceramic coatings on metal or ceramic substrates at relatively low temperatures. Cold Spray has moved from a scientific curiosity to a now established and integrated manufacturing process relatively quick. Special material powders with specific characteristics, required for cold spray processing are readily available. Today, Cold Spray systems are being utilized in a wide range of applications including performance-enhancing coatings, protective layers, manufacturing new components, and repairing fabricated parts. The number of industries adapting to cold spray technology is increasing, from aerospace, automobile, turbine, and defense industries to name a few.

History

Cold spray has been around for some time, this process was mentioned over a century ago. In 1900, Thurston [2] filed a patent for a method in which metal particles are thrown upon against a metal plate by a blast of pressurized gas with significant force to cause the particles to become embedded by plastic deformation in the surface of the metal body and to form a permanent coating.

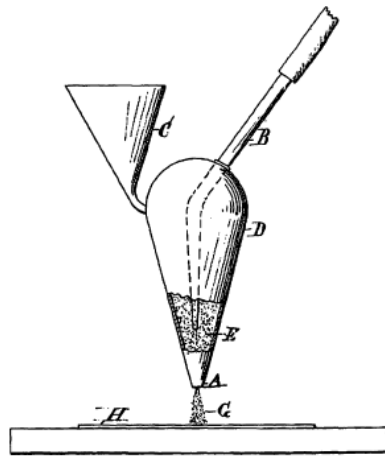


Figure 1: Schematic of Thurston's design [2]

In 1958, Rocheville [3] filed a patent to protect a device that mostly uses the method patented by Thurston but using a De Laval type nozzle with high-pressure air to propel the fine powder particles at a higher velocity to form a coating. In his method, powder particles were powered by the supersonic blast of air directed against a substrate, and as a result, the powder adheres to the surface where it is firmly retained. This is a thermal spray that is an all-solid-state coating working only with the principle of plastic deformation of the particle upon impact. Rocheville mentioned that a thin uniform layer is formed over the entire surface. The coating is built up only over the surface of the part but not upon the coat itself. Even with the use of a supersonic nozzle the device, Rocheville could not propel the

particles to high enough velocities to produce thick layers on a substrate. Critical velocity is a big factor when it comes to the desired thickness of the coating, ideally you want the velocity to be in the range of 300 to 600 meters per second, which is greater than the speed of sound. The speed of sound for air at 300 K is around 347 m/s.

In the 1980s, after a couple of decades of cold spray technology being left alone it picked up some interest from a group of scientists at the Institute of Theoretical and Applied Mechanics of the Siberian Division of the Russian Academy of Sciences in Novosibirsk, Russia. They performed supersonic wind tunnel tests to study two-phase flow around bodies using small tracers in the flow. With the use of tracers in the tests, they were able to establish and use a critical velocity, that if exceeded would create a transition from particle erosion of the target surface to rapidly increasing deposition. Although some others had observed the phenomenon of “gas dynamic cold spray”, the Russians developed the process as a coating technology.

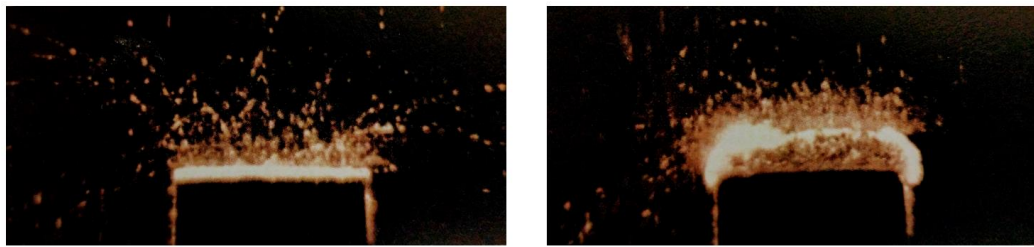


Figure 2: Early Russian Tunnel Experiments (a) Copper particles at 250m/s: Erosion (b) Copper particles at 900m/s: Deposition [4]

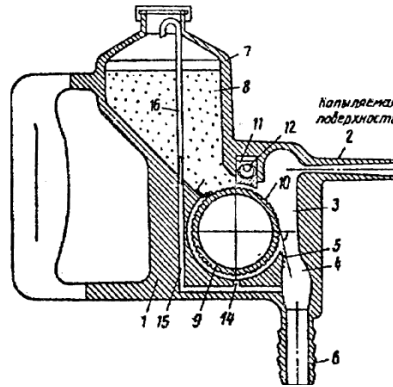


Figure 3: The First device for applying a coating by cold spray patented in 1986 [4]

Working Principle

The principle of cold spray is based on the metal particle deformation behavior during high-velocity impact with a solid substrate. In the process, the propellant gas is accelerated to supersonic velocity in a convergent-divergent (de 'Laval) nozzle. The coating powdered material is injected into the gas stream, stimulated by the propellant gas in the nozzle, and propelled towards the substrate to be coated. If the impact velocity of the particle exceeds a specific critical value, the impact energy from the particle provokes an intense plastic deformation of the particle. Upon impact, the particle breaks into a thin film on the substrate which helps to establish intimate, clean contact between the particle and substrate which leads to the creation of intense bonding. Hence, a dense and solid adhesive coating on the substrate surface is formed [10].

The main components of Cold Spray system include:

- Powder feeder
- Propellant Gas
- Gas heater to preheat the gas

- Supersonic nozzle
- Spraying chamber with a motion system
- Method for controlling spray parameters

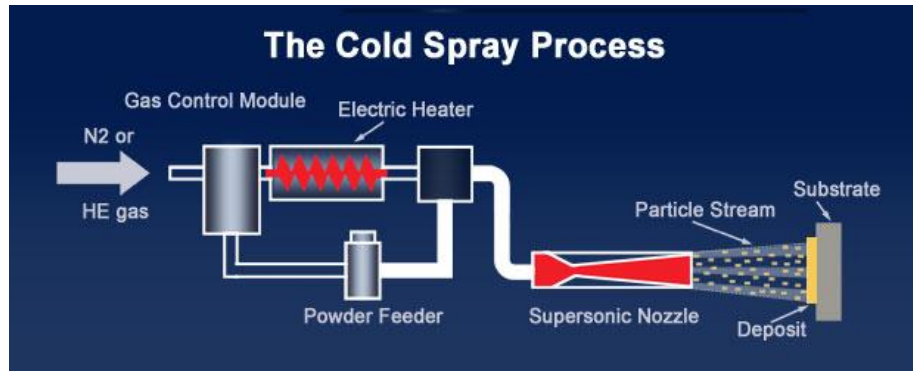


Figure 4: Cold spray system component example

The equipment used for cold spray has been continuously developed to achieve optimum impact conditions for a large variety of materials. Materials that have low melting temperatures can be successfully deposited by moderate conditions, using less expensive low pressure/temperature equipment. There is a necessity of having the more powerful hardware for providing higher pressures and temperatures for processing high strength materials.

Various thermal spray techniques are compared with cold spray and discussed at more detail in terms of impact velocity and temperature by Ang. [9]. In the particle temperature and velocity map, one can observe that the process temperature of cold spray

technology is much lower than 1000 °C and impact velocity can get much higher than 1000 m/s when compared with other thermal spray processes.

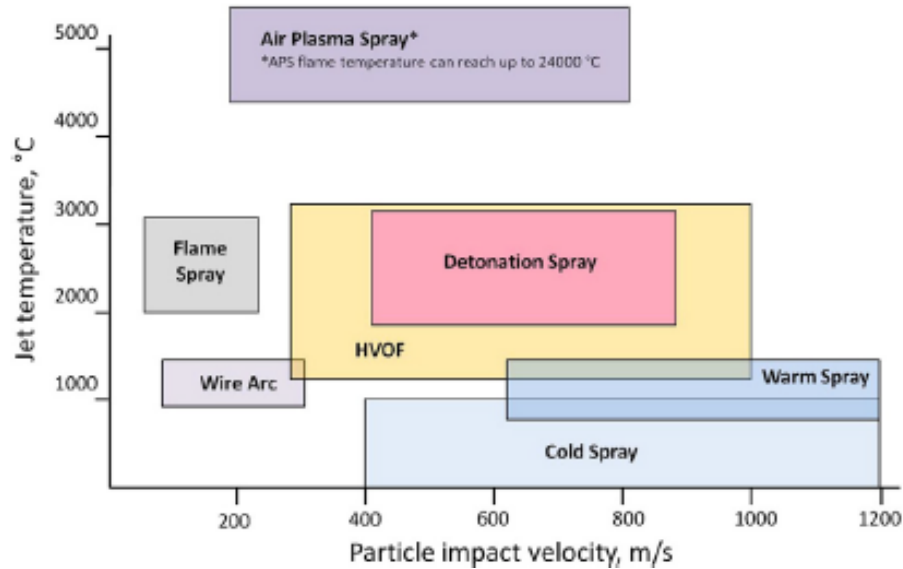


Figure 5: Particle temperature and velocity map [7]

Cold Spray Systems

A Cold Spray System can be designed in fixed, manual, portable, or robotic systems.

There are two main categories of cold spray systems:

1. Low-Pressure Cold Spray System,
2. High-Pressure Cold Spray System

1 Low-Pressure Cold Spray System (LPCS)

In the Low-Pressure cold spray system (LPCS) , the powder is injected in the diverging section of the nozzle where the gas is expanded [5]. Atmospheric pressure air is supplied to transport powder from the feeder. Hence, the LPCS does not require a

pressurized feeder. LPCS is typically smaller and often found in portable systems. The range of particle velocities that can be achieved through this system usually ranges between 300 to 600 m/s. They are used for the application of lighter materials and are generally available with air or nitrogen as a propellant gas at pressures on the order of 0.5 to 1.0 MPa.

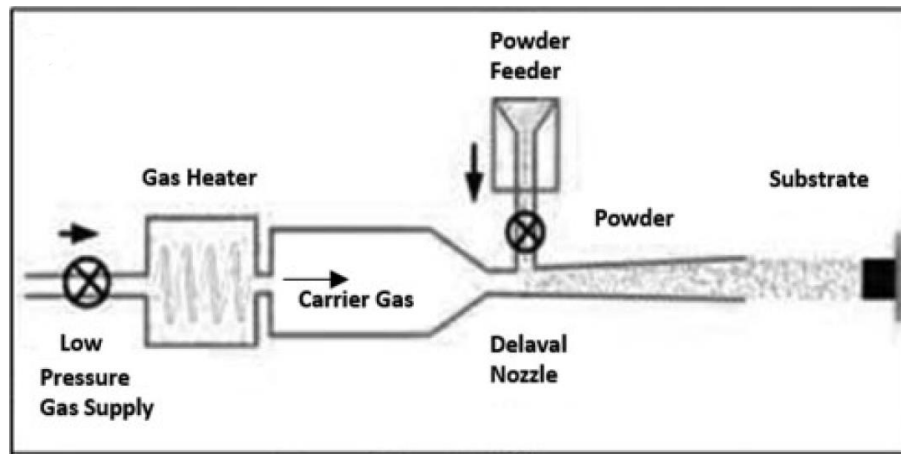


Figure 6: Low-Pressure Cold Spray system [6]

2 High-Pressure Cold Spray system (HPCS)

In High-Pressure Cold Spray, small particles can generate relatively higher particle velocities compared to LPCS ranging from 800 to 1400 m/s. Lower density gasses like helium or nitrogen are usually preferred for this system. The speed of sound for nitrogen and helium at 20°C & 1 atm are 349 m/s and 1007 m/s. The gases are pressurized high, typically high in the range of 1 to 5 MPa through the converging-diverging nozzle to achieve high particle impact velocities.

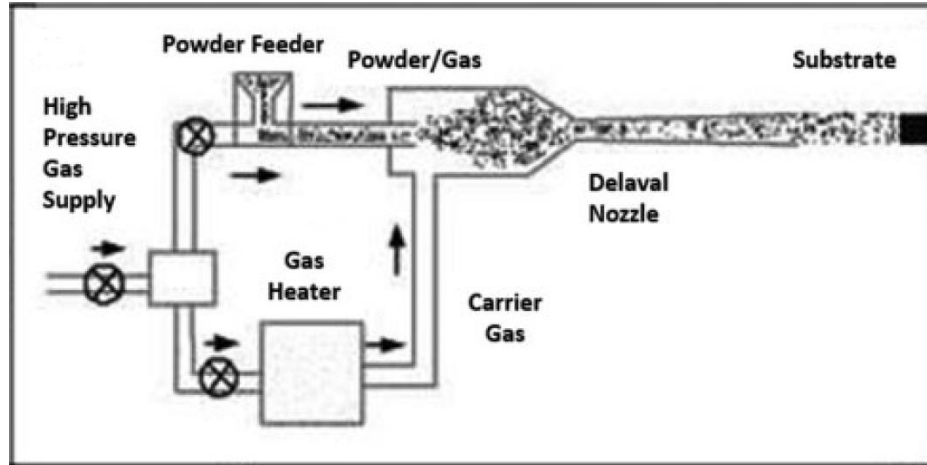


Figure 7: High-Pressure Cold Spray system [6]

For HPCS, high-pressure powder feeder running at a higher pressure than main gas stream is required to avoid powder backflow. High-pressure powder feeders are usually very expensive and large in size. Nozzle clogging is the other major problem with HPCS. When the particle velocity and temperature are increased, it can get worse. To overcome this problem, either a larger than average particle diameter is needed or a higher yield strength second particle population should be mixed with the first particle population [7]. Due to particle erosion, severe wear will occur at the nozzle throat which affects the operation of the nozzle and leads to more considerable variations in deposit quantity. It gets worse when particles of harder material are sprayed. On the other hand, the LPCS has the simpler equipment, however, LPCS can only achieve relatively fewer particle velocities compared to HPCS as the exit Mach number and inlet pressure is low, usually below 1 and 3 MPa respectively. Otherwise, the atmospheric pressure would no longer be able to supply powders into the supersonic nozzle.

Cold Sprayed Coatings

Cold spray offers many technical benefits when compared with other coating processes. Because cold spray does not use a high-temperature heat source, such as a flame or plasma, to melt the feed material, it does not deposit large amounts of heat into a coated sensitive coating material through oxidation or other in-flight chemical reactions. For this reason, cold spray seems very attractive for depositing oxygen-sensitive materials, such as copper or titanium.

Other properties include

- No powder melting
- No grain growth
- No phase changes
- No oxidation
- High dense coatings
- Low porosity
- High thermal conductivity
- High electrical conductivity
- Corrosion resistant
- High bond strength
- High compressive residual stress.

Similarly, cold spray offers exciting new possibilities of building thick coatings and even free-standing shapes, from Nanophase materials, intermetallic, or amorphous materials.

Coating materials include:

Used to produce dense, pure, thick and well bonded deposits of many metals and alloys, such as Aluminum (Al), Copper (Cu), Nickel (Ni), Silver (Ag), Tantalum (Ta), Pure titanium (Ti), Zinc (Zn), Stainless steel, Nickel based alloys (Hastalloys, Inconel), and Bondcoats such as MCrAlYs

Manufacturing Advantages

- No masking is required for this process
- Flexibility in substrate
- Dissimilar materials can be coated on a substrate
- High Deposition efficiency can be obtained
- Ultra-thick coatings can be produced

Limitations

- Significantly less ductility
- Line of sight
- Limited sprayable materials
- The substrate must be hard enough
- High gas consumption

Applications of cold spray technology

Thermally sprayed coatings are usually evaluated by considering: 1) Adhesion to the substrate; 2) Porosity; and 3) Oxide contents in the layer. Presently cold spray enables the obtainment of coatings characterized by very low porosity, oxide content, and high

adhesion. Also, the lack of thermal stress in the layer and substrate increases the spectrum of cold spray method application in comparison with other thermal spraying methods. Cold spray can be used for applying coatings on most engineering materials. Cold spray applications are vast and primarily includes the following areas:

Coatings

- Oxidation protection coatings
 - Copper-chrome layers
- Corrosion resistant coatings
 - Aluminum and zinc
- Composites
 - Metal-metal: copper-tungsten
 - Metal-carbide: aluminum-silicon carbide
 - Metal-oxide: aluminum-alumina
- Wear-resistant coatings
- Fretting Fatigue resistant coatings
- Self-lubrication coatings
- High-temperature protection coatings

Repairs and restoration in the following industries

- Aerospace

- Agriculture
- Automotive
- Tooling

Essential Parameters to be controlled in Cold Spray

To meet strong bonding, setting up the process, and powder parameters are vital. The following are the significant parameters to be monitored in a typical Cold Spray system:

- *Impact conditions*: Impact velocity, Impact temperature
- *Nozzle design*: Nozzle Throat diameter, Nozzle Exit diameter, Convergent length, Divergent Length and Profile Shape
- *Propellant Gas*: Gas temperature, pressure and Gas type
- *Particle*: Particle Velocity, Particle Temperature, Particle Size, Particle type and Critical Velocity of the particle
- *Substrate*: Standoff distance, Substrate temperature, Substrate type
- Deposition Efficiency

Modeling and simulation of Cold Spray

To ensure optimized and successful cold spraying, the influence of various processes, powder parameters on the critical velocity, and deposition efficiency should be well understood. Application of modeling and simulation in cold spray research is a feasible and robust way to reach this goal. Works related to modeling of the cold spray powder spraying process cover two primary research areas, i.e., modeling of powder particle deformation and modeling of powder particle velocity. Other research areas include modeling of substrate heating and building up residual stress in cold spraying. [11]

The numerical simulation of gas/powder velocity enables the determination of the gas state parameters inside the nozzle and once the gas has left it as well as the distribution of powder particle velocity and temperature.

Particle velocity is an important factor that determines whether particles can adhere on the substrate surface. It is known that particle in flight velocity is highly dependent on the character of the gas flow field inside and outside the nozzle because the powders are only dragged and accelerated by the compressed driving gas during the process. As for the gas flow field, it is influenced by several factors, including operating parameters, nozzle geometry, and standoff distance. Therefore, to achieve a high particle impact velocity, a large body of works has been carried out to optimize the parameters of nozzle geometry and operating parameters, and the following flow field. Among these studies, Computational fluid dynamics (CFD) technique was always adopted to predict the gas flow field and particle velocity due to its lower cost and lower time consumption compared to experimental implementations.

CHAPTER 2: LITERATURE REVIEW

This chapter contains a literature review related to the optimization of various parameters of the cold spray process and internal profile of the De Laval nozzle used for the cold spray process. The study done in this thesis is aimed to add more knowledge on cold spray simulation and to solve potential problems or questions not answered by the literature available on cold spray technology.

The exponential increase of industrial demand over the past two decades has led scientists to develop alternative technologies for the fast manufacturing of engineering components, in addition to standard time-consuming techniques such as casting or forging.

W. Li [28] covered the coloration between the different turbulence models he used and the meshing differences. He had various plots on velocity relations with different parameters, these studies were informative and insightful on how the copper particles behaved when impinged on a low carbon steel substrate. He confirmed the established theory of what the ideal critical velocity should be to create adequate bonding and the parameters that simulations must achieve with particle velocity and temperature in mind in order to get adequate and desired results in additional studies.

X.K. Suo [33] performed a numerical study on the effect of nozzle dimension on particle distribution in cold spraying. In his analysis, he systematically changed the height of rectangular nozzle's exit, throat, and powder injector; keeping nozzle expansion ratio as a constant to study their effects on the distribution and velocity of magnesium particles using three-dimensional models of cold spraying systems. He also examined the effect of particle size on the particle distribution. He found that the particle distribution is mainly

influenced by the turbulent kinetic energy of the gas flow at the nozzle exit. He also showed that changing the height of the exit or throat can control the particle distribution, i.e.; 1) As the exit height increases, the particle distribution broadens and flattens along the transverse direction; 2) As the throat height increases, the particle distribution becomes sharp, and the mean particle velocity decreases along the transverse direction; 3) As the powder injector height increases, the mean particle velocity increases.

Wen-Ya Li [15] designed a convergent barrel cold spray nozzle through numerical simulation. He found that the main factors influencing are particle velocity and temperature including the length and diameter of the barrel section, nature of the accelerating gas, pressure, and temperature of the accelerating gas, and the particle size. His analysis showed that under constant gas pressure, particles could achieve high temperature but relatively low velocity when the convergent-barrel nozzle is used compared to a convergent-divergent nozzle. His experiments with copper powder using convergent-barrel nozzle confirmed the feasibility to deposit thick, dense coating under a low gas condition.

J. Villafuerte [29] covers a basic background on modern ways cold spray technology is being used. This paper is useful to give a more detailed background on how cold spray works and its advantages and disadvantages. It discusses about the modern industry and how the cold spray technology keeps advancing due to its benefits in deposition on fragile materials.

T. Schmidt [31] covered how the parameters of bonding occur based on the material properties that varied. The bonding of the particles onto the substrate can be calculated theoretically and simulated importing the solid mechanics characteristics into a fluid dynamic program like Fluent. The focus was on measuring the ideal conditions looking at

the window of deposition. That determined you must be within the window of deposition to achieve ideal bonding because if exceeded the particles erode and if not reached the particles would not bond properly on the substrate.

M. Meyer [19] experimented with three different nozzle designs under constant conditions and simulated their performance using Ansys v14.0. The deposition efficiency was measured using titanium as a feedstock material, and it was shown that it decreases with the cross-sectional throat area of the nozzle. He found that one-way coupled multiphase results could not agree with his experiments whereas more sophisticated modeling techniques with two-way couplings could partially provide high-quality outcomes.

S. Yin [20] investigated the effect of carrier gas temperature on the particle acceleration and deposition by both numerical and experimental methods. He found that the carrier gas temperature significantly influences the supersonic driving gas flow and the resulting particle acceleration. The velocity and temperature of the driving gas at the throat and divergent section of the nozzle exhibit an increasing trend with gas temperature.

His results showed that higher carrier gas temperature results in increased particle velocity as well as the final impact temperature. From his analysis, it found out that the particle impact velocity is more influential than critical velocity reduction.

M Karimi, [21] presented a computational fluid dynamics model of the cold gas-dynamic spray process. The gas dynamic flow field and particle trajectories within an oval-shaped supersonic nozzle as well as in the immediate surrounding of the nozzle exit, before and after the impact with the target plane are simulated. Their predicted values of the

particle nozzle wall pressure compare well with experimental data. Their works showed that the particle distribution is considerably asymmetric about the major axis but relatively symmetric about the minor axis. Their preliminary wear pattern on the nozzles sides supports this finding. Details of the particle release pattern into the surroundings are conveniently depicted. However, their works underestimated velocity magnitudes.

R. Lupoi and O'Neill [22] investigated the powder stream characteristics in cold spray supersonic nozzles. In his experiment, he varied the powder insertion location within the carrier gas flow, along with the geometry of the powder injector, to identify their relationship with particle trajectories. R. Lupoi performed the experiment as well as CFD simulations for his analysis. He used Fluent v6.3.26 for running CFD simulation and results obtained compared to the experimental results. He modeled and tested for configurations with various acceleration channel lengths, powder injector geometry, and locations. They found out that when the powder is released axially and upstream from the nozzle throat, particle trajectories do not stay close to the centerline, but tend to spread over the entire volume of the channel. Their CFD analysis has shown that the leading causes for this effect are a relatively high gas turbulence level generated at the vicinity of the nozzle throat, which affects particle trajectories and particle deflections due to impacts against channel walls. They also found that by employing a smaller diameter injector, a narrower beam can be achieved.

X.K. Suo [23] performed a numerical study on the effect of nozzle dimension on particle distribution in cold spraying. In his analysis, he systematically changed the height of rectangular nozzle's exit, throat and powder injector keeping nozzle expansion ratio as a constant to study their effects on the distribution and velocity of magnesium particles

using three-dimensional models of cold spraying systems. He also examined the effect of particle size on the particle distribution. He found that the particle distribution is mainly influenced by the turbulent kinetic energy of the gas flow at the nozzle exit. He also showed that changing the height of the exit or throat can control the particle distribution, i.e.; 1) As the exit height increases, the particle distribution broadens and flattens along the transverse direction; 2) As the throat height increases, the particle distribution becomes sharp, and the mean particle velocity decreases along the transverse direction; 3) As the powder injector height increases, the mean particle velocity increases.

M Grujicic [24] used the one-dimensional isentropic model to analyze the dynamics of dilute two-phase flow during the cold spray process. His obtained results show that there is a particle velocity dependence, carrier gas invariant optimal value of the relative gas or particle Mach number that maximizes the drag force acting on feed powder particles, hence maximized the particle acceleration. He found that to increase the average velocity of the particles at the nozzle exit; the gas dynamic cold spray nozzle is designed in such a way that at each axial location, the acceleration of the particles is maximized. He showed that the exit velocity of particles could be substantially increased when helium is used as the carrier gas.

Muhammad Faizan Ur Rab [25] developed a three-dimensional CFD multicomponent model to estimate cold spray gas conditions involving both nitrogen and air. He claimed that the developed holistic model is useful in determining the state of gas and particles from injection point to the substrate surface with the advantage of optimizing very rapid cold spray deposition in nanoseconds. He utilized the two-equation $k-\epsilon$ model for developing the three-dimensional numerical model. The model was tested and validated

with temperature parameter measured experimentally for a titanium substrate. He showed that the multicomponent model could be identified as a realistic model for cold spray process revealing the information about the complex thermos-mechanical events concerning gas temperature, velocity and turbulence kinetic energy from gas inlet to the location, at which the supersonic jet impinges onto the substrate.

A. Karaoglanli [33] carried out different material layers to see their effects on mechanical properties. They first created a metallic coating and then added a ceramic coating over it making the deposition of materials more complex. They observed that the void and porosity of the bottom layer decreased due to the top layer deposition compressing the bottom layer on impact as expected. Conclusion is that multi-layer deposition would increase the mechanical properties to create a better deposition in the layer of the coating.

R.Lupoi [26] presented deposition efficiency (DE) results from different supersonic nozzles when using titanium as the feedstock material. He carried out a theoretical analysis through computational fluid dynamics to compare numerical results against experimental findings. For running CFD simulations, he used Fluent v14.0 solver. He manufactured four nozzles with different internal profiles and tested them using the same processing conditions with titanium powder. His results have suggested that current commercial codes cannot accurately predict the acceleration process under realistic working conditions.

Chang-Jiu Li [27] theoretically examined the deposition behavior of a spray particle stream with a particle size distribution regarding deposition efficiency as a function of spray angle and parameters of the particle. He conducted few experiments where he has measured the deposition efficiency at different driving gas conditions and spray angles using copper powder. His analysis revealed that the particle velocity distribution resulting

from particle size distribution significantly influences the deposition efficiency in cold spraying. He proposed a formula to calculate the deposition efficiency using the modified Rosin-Rammler model of particle size distribution and the relation between the size and velocity of the particle. His works established a theoretical relationship between the deposition efficiency and spray angle to explain the effect of off-normal spray angle on the deposition efficiency in cold spraying when the impact of the tangential component of the velocity on particle deposition was neglected.

Research Objective

Research has been done in this field looking at simulating the flow going through the cold spray nozzle, but the particle behaviour has not been investigated. In this study, the behaviour of the particles will be observed in a stepped drilled nozzle and examine the effects caused by the different parameters. In actual application, many industries use step drilled nozzle for its cheaper design and manufacturing cost. There are no research studies performed on determining the effects of step drilled nozzle numerically. In this study, as a first approximation, a numerical investigation is conducted on a step drilled nozzle design with the same operating parameters except the number of particles injected and the use of two different carrier gases such as nitrogen and helium. The proper procedures to make particle injection simulations will be explained and broken down for future research on this topic.

CHAPTER 3: METHOD AND APPROACH

Methods and techniques used in the modeling and simulation of various cold spray nozzle CAD models and CFD analysis are discussed in this chapter.

Methodology

- Problem Statement
- Geometry
- CAD Model Generation
- Discretization
- Physics
- Solution
- Visualization
- Validation

Problem statement

The problem addressed in this research is:

How to properly create supersonic jet particle simulations and observe the behavior of particles in a cold spray system when tested in various parameters in a Step Drilled nozzle

Geometry

Step Drilled Nozzle

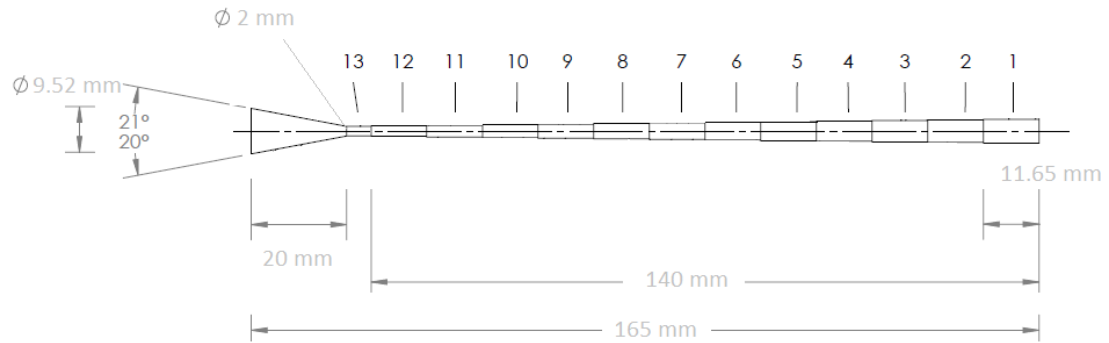


Figure 8: Step Drilled Nozzle Geometry

	Diameter (mm)	Step length (mm)
Step 1	4.97	11.65
Step 2	4.69	11.65
Step 3	4.49	11.65
Step 4	4.21	11.65
Step 5	3.98	11.65
Step 6	3.73	11.65
Step 7	3.45	11.65
Step 8	3.25	11.65
Step 9	2.94	11.65
Step 10	2.69	11.65
Step 11	2.43	11.65
Step 12	2.18	11.65
Step 13	2	Remainder

Table 1: Step Drilled Nozzle Step Dimensions

Summary of the Geometrical Dimensions

	Nozzle 1
Inlet Diameter (mm)	9.52
Outlet Diameter (mm)	4.97
Throat (mm)	2
Convergent Length (mm)	20
Divergent Length (mm)	145
Divergent Profile (mm)	Stepped
Stand Off Distance (mm)	20

Table 2: Summary of Nozzle Dimensions

CAD Model Generation

CAD Models of the Geometries provided in the geometry section are generated using the StarCCM+ software. The operational procedure for CAD Modeling in StarCCM+ is briefly discussed in Chapter 4.

Nozzle 1 (Step Drilled)

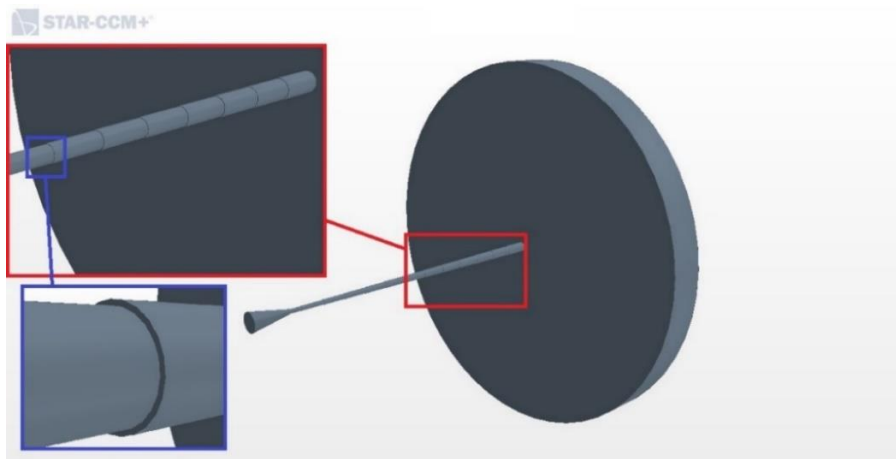


Figure 9: Step Drilled Nozzle CAD Model

Discretization

There are numerous methods of discretization, which can broadly be classified into a mesh (grid) methods and mesh-free methods. Mesh methods are more widely used. In the Meshing process, the region is divided into smaller areas. These smaller regions may be of different shapes like triangles, rectangles in case of 2D geometry, hexahedrons, tetrahedrons in case of 3D geometry. Then, the governing equations are discretized over the mesh. Finite Difference Method, Finite Element Method, and Finite Volume Method are very popular methods of discretization in Computational Fluid Dynamics.

Meshing models used for the simulation

- Extruder
- Advanced Layer Mesher
- Surface Wrapper
- Surface Remesher

Instructions for setting up the meshing in Starccm+ is provided in Chapter 4

Nozzle 1 (Stepped Nozzle)

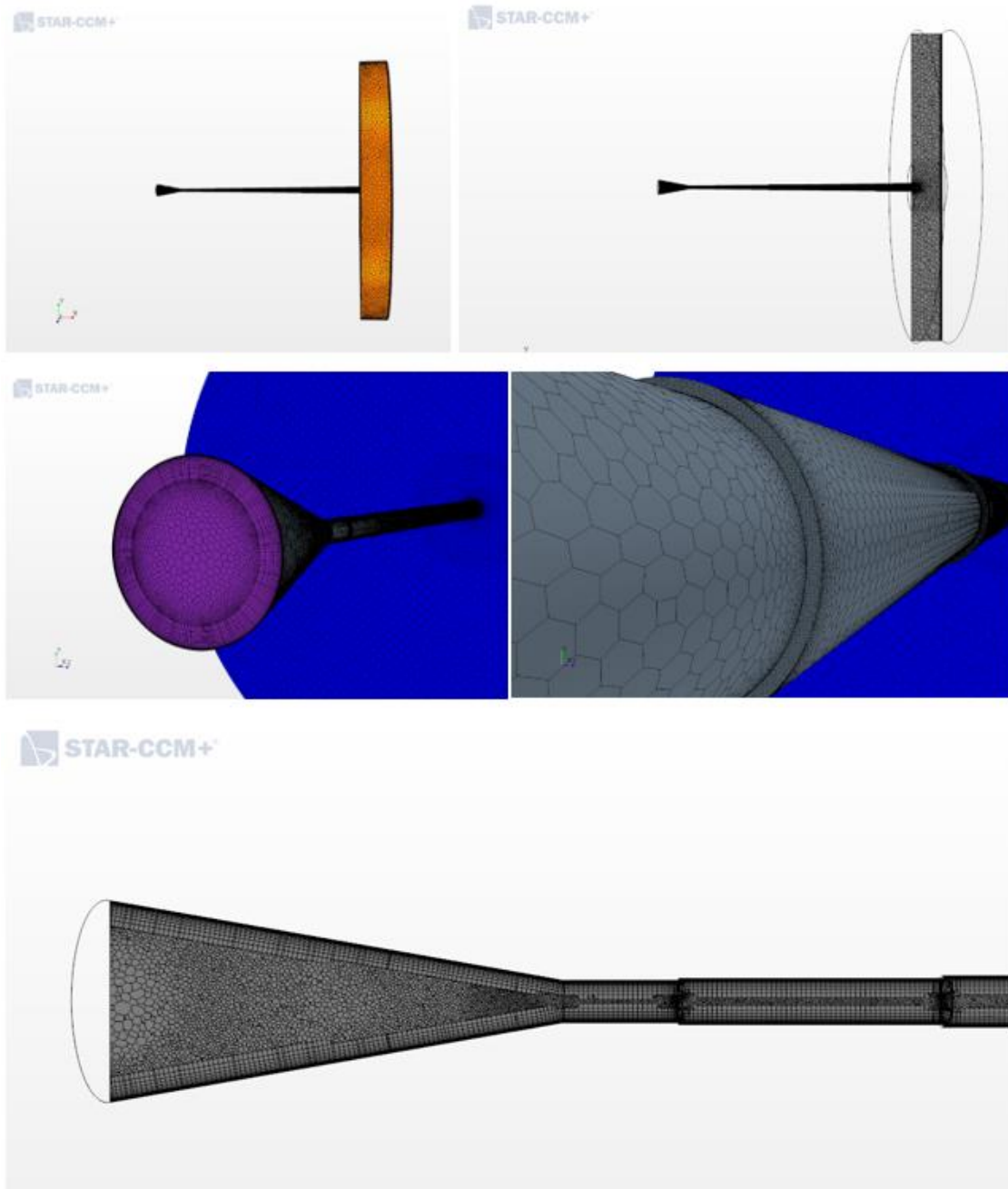


Figure 10: Step Drilled Nozzle Mesh

Number of Cells: ~1,283,558 Number of Face: ~6,479,006

Physics

Nozzle throat is referred to the smaller cross-section area of the converging/diverging nozzle. The gas temperature at nozzle throat (T^*) is defined as

$$\frac{T_0}{T^*} = 1 + \frac{\gamma - 1}{2}$$

$$T^* = \frac{T_0}{1 + \frac{\gamma - 1}{2}}$$

Gas velocity at nozzle throat (V^*) is defined as

$$V^* = \sqrt{\gamma R T^*}$$

The mass flow rate (\dot{m}) of the sonic gas can be defined by

$$\rho^* = \frac{\dot{m}}{V^* A^*}$$

The gas pressure at the nozzle throat can be determined using the ideal gas law:

$$P^* = \rho^* R T^*$$

The stagnation pressure at the nozzle throat can be defined using the isentropic relations

$$\frac{P_o}{P^*} = \left(\frac{T_0}{T^*} \right)^{\frac{\gamma}{\gamma-1}}$$

$$\frac{P_o}{P^*} = \left(1 + \frac{\gamma - 1}{2} \right)^{\frac{\gamma}{\gamma-1}}$$

$$P_o = P^* \left(1 + \frac{\gamma - 1}{2} \right)^{\frac{\gamma}{\gamma-1}}$$

Once the parameters at the throat are defined, it is possible to determine these quantities along the diverging section of the nozzle. When the variation of the nozzle cross-sectional area is specified, the corresponding Mach number (M) can be determined using the following equation

$$\frac{A}{A^*} = \left(\frac{1}{M}\right) \left[\left(\frac{2}{\gamma + 1}\right) \left(1 + M^2 \frac{\gamma - 1}{2}\right) \right]^{\frac{\gamma + 1}{2(\gamma - 1)}}$$

Once the Mach number is obtained at a given cross-sectional area of the diverging nozzle section, the remaining corresponding values can be determined by using the following isentropic relations

$$\frac{P}{P^*} = \left(\frac{\gamma + 1}{2 + (\gamma - 1)M^2} \right)^{\frac{\gamma}{\gamma - 1}}$$

$$P = P^* \left(\frac{\gamma + 1}{2 + (\gamma - 1)M^2} \right)^{\frac{\gamma}{\gamma - 1}}$$

$$\frac{T_o}{T} = 1 + \frac{\gamma - 1}{2} M^2$$

$$T = \frac{T_o}{1 + \frac{\gamma - 1}{2} M^2}$$

$$\frac{\rho_o}{\rho} = \left(1 + \frac{\gamma - 1}{2} M^2 \right)^{\frac{1}{(\gamma - 1)}}$$

$$\rho = \frac{\rho_o}{\left(1 + \frac{\gamma - 1}{2} M^2 \right)^{\frac{1}{(\gamma - 1)}}}$$

Governing equations

The flow in cold spray is considered as steady-state supersonic turbulent flow with heat transfer during the process.

The governing equations are:

- Continuity equation
- Momentum equation
- Energy equation

Continuity equation:

$$\frac{\partial \rho}{\partial t} + \frac{\partial}{\partial x_i} (\rho u_i) = 0$$

Momentum Equation:

$$-\frac{\partial(\rho u_i)}{\partial t} + \frac{\partial(\rho u_i u_j)}{\partial x_j} = -\frac{\partial P}{\partial x_i} + \left[\frac{\partial \tau_{ij}}{\partial x_j} \right]$$

$$\tau_{ij} = \mu \left[\frac{\partial u_i}{\partial x_j} + \frac{\partial u_j}{\partial x_i} - \frac{2}{3} \frac{\partial u_k}{\partial x_k} \delta_{ij} \right]$$

Energy Equation:

$$\frac{\partial \rho E}{\partial t} + \frac{\partial}{\partial x_j} (\rho E u_j) = \frac{\partial \tau_{ij}}{\partial x_j} u_i + \frac{\partial}{\partial x_j} \left(k \frac{\partial T}{\partial x_j} \right)$$

Particle Equations

Conservation of linear momentum:

$$m_p \frac{d\mathbf{v}_p}{dt} = \mathbf{F}_s + \mathbf{F}_b$$

Resultant forces on particle surface:

$$\mathbf{F}_s = \mathbf{F}_d + \mathbf{F}_p + \mathbf{F}_{vm}$$

Resultant forces of the body force:

$$\mathbf{F}_b = \mathbf{F}_g + \mathbf{F}_{MRF} + \mathbf{F}_u + \mathbf{F}_c + \mathbf{F}_{Co}$$

Turbulence Model Equations

Reynolds-Averaged Navier-Stokes equations:

$$\phi = \bar{\phi} + \phi'$$

Mean mass, momentum and energy transport Equation:

$$\frac{\partial}{\partial t}(\rho \bar{E}) + \nabla \cdot (\rho \bar{E} \bar{\mathbf{v}}) = -\nabla \cdot \bar{p} \bar{\mathbf{v}} + \nabla \cdot (\bar{\mathbf{T}} + \mathbf{T}_{RANS}) \bar{\mathbf{v}} - \nabla \cdot \bar{\mathbf{q}} + \mathbf{f}_b \bar{\mathbf{v}}$$

$$\mathbf{T}_{RANS} = -\rho \begin{pmatrix} \overline{u'u'} & \overline{u'v'} & \overline{u'w'} \\ \overline{u'v'} & \overline{v'v'} & \overline{v'w'} \\ \overline{u'w'} & \overline{v'w'} & \overline{w'w'} \end{pmatrix} + \frac{2}{3} \rho k \mathbf{I}$$

Solver Settings

Fluid motion equations are generally very complex and frequently require computational ways to solve. The CFD program solves the Navier-Stokes equations for compressible flow. In this study, CFD simulations were performed using STAR CCM+ to predict the gas flow field.

Selected Physics Models for the simulation

- Three Dimensional
- Constant Density
- Implicit Unsteady State
- Discrete Element Model (DEM)
- Lagrangian Multiphase
- Multiphase Interaction
- Proximity Interpolation
- Fluid: Gas (Air, Nitrogen, or Helium)
- Ideal Gas
- Reynolds Averaged Navier Stokes
- Coupled Flow
- Coupled Energy
- Turbulent Flow
- SST K – Omega
- Turbulence Suppression
- Transition Boundary Distance

- All y^+ Wall Treatment
- Exact Wall Distance
- Gradients

Setting up physics models with Star CCM+ is briefly discussed in Chapter 4.

Boundary Conditions

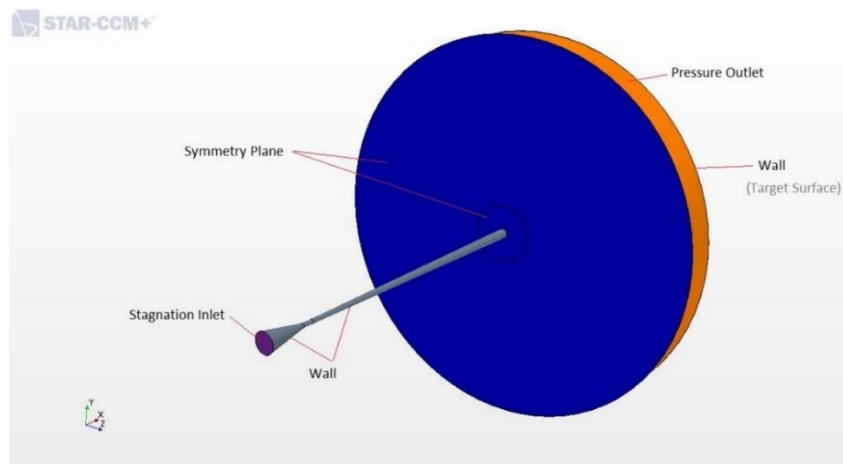


Figure 11: Model Showing Boundary Conditions

Summary of Boundary Conditions used for various nozzles

	<i>Step Drill Nozzle</i>
Stagnation Inlet	Nozzle Inlet
Pressure Outlet	Radial Outlet
Symmetry Plane	Top1, Top2
Wall	Convergent, Divergent

Table 3: Summary of Boundary Conditions used for the Nozzle

CHAPTER 4: RESULTS AND DISCUSSION

In this Chapter, we will observe the creation and behavior of the particles, the obtained results from the numerical simulations will be visualized and validated. The breakdown of the steps needed to create the supersonic jet particle simulation will be demonstrated. Then visualization will be broken down into two areas: a scalar cross-section view of the gas flow and the scalar field of the particles. Finally, we will be observing how the different carrier gasses affect the flow and the particle behavior.

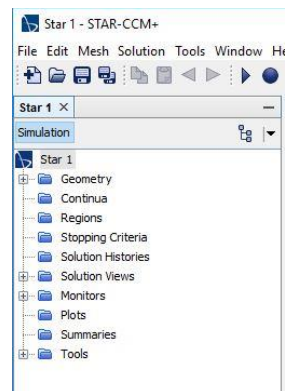
Simulation procedure in Star CCM+

The instructions with pictures provided below will briefly go through the steps of running a successful CFD particle simulation in Star CCM+ software.

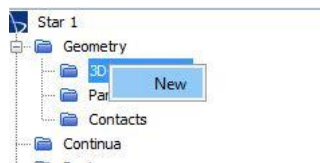
Step 1: Click Create a file

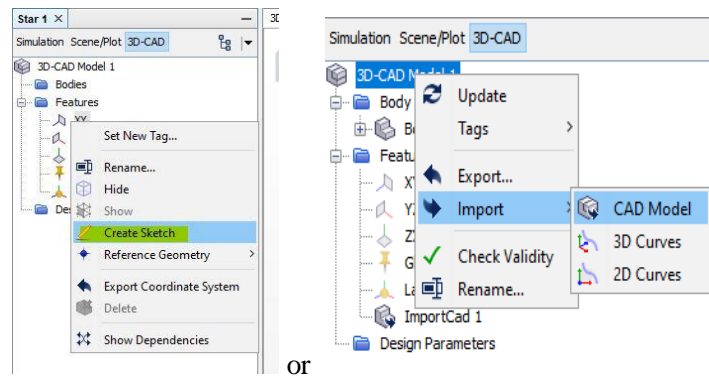


Select the type of processor and click OK. The file structure will be created.

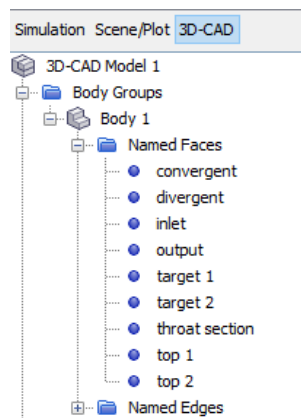
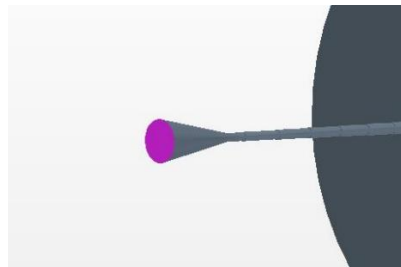


Step 2: Create or import CAD Geometry

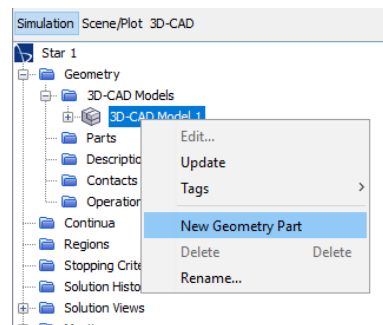


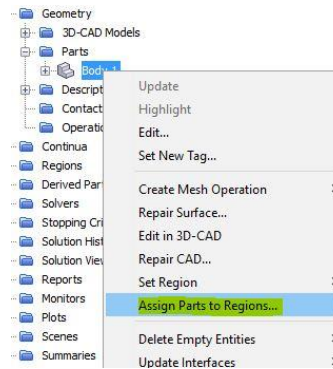
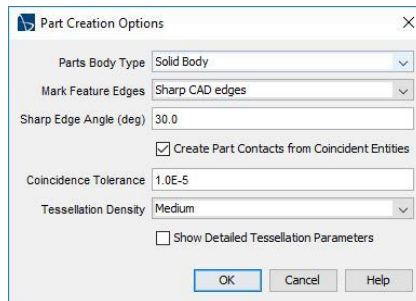


Step 3: After building the 3D CAD model, name the faces of the CAD.



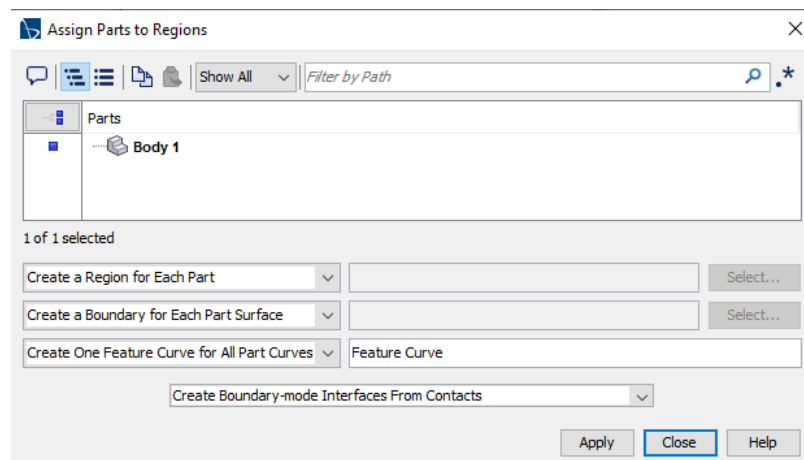
Step 4: Create Regions for the CAD Model



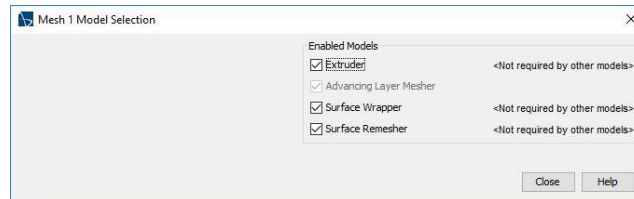
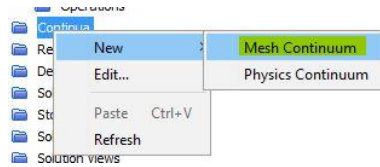


Specify to create a region for each part and a boundary for each part surface

(note: press Apply button only once even if nothing populates)

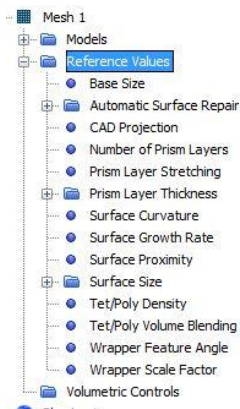


Step 5: Select Meshing Models



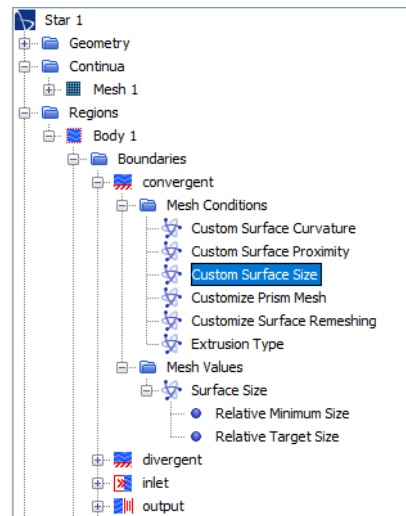
Step 6: Set Mesh control variables properly

Adjust base size (Decrease) and number of prism layers (Increase)



Step 7: Use custom meshing on more intrigued boundaries for better meshing

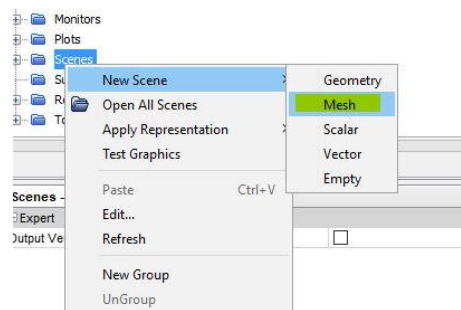
Adjust Relative Minimum size and Relative Target size for each boundary



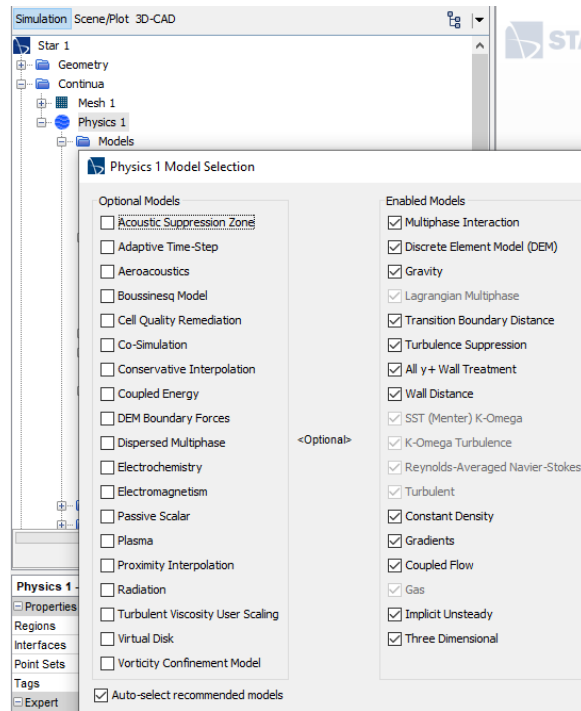
Step 8: Click the 'Meshed Cube' to perform meshing the CAD model



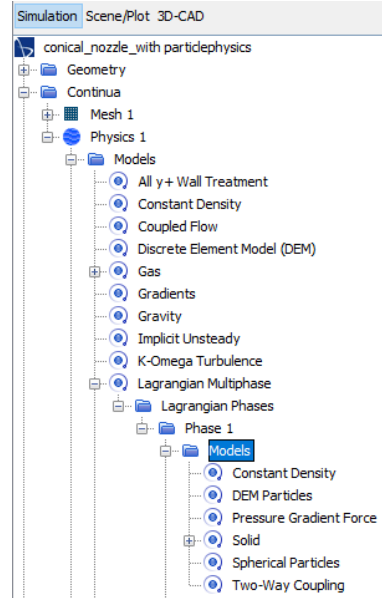
Step 9: Create a new Mesh scene to visualize the mesh

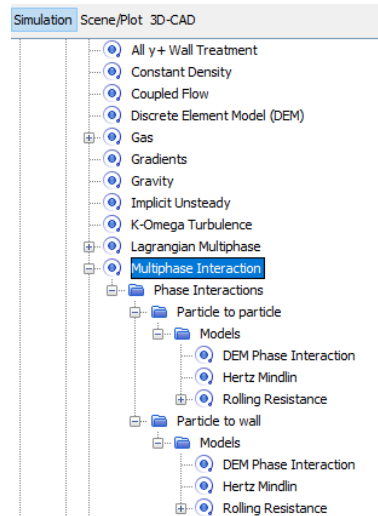


Step 10: Select Physics models

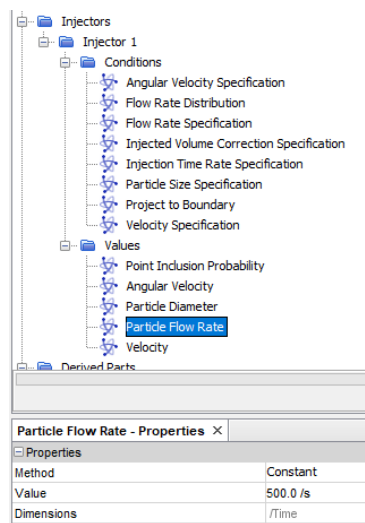
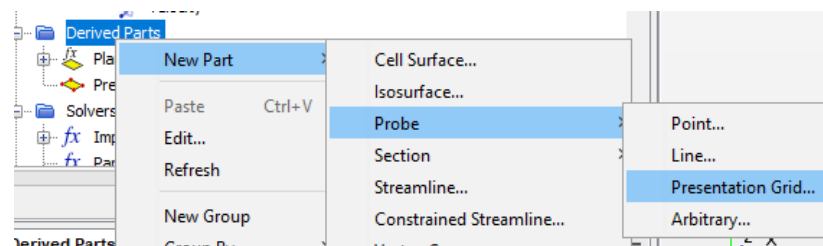


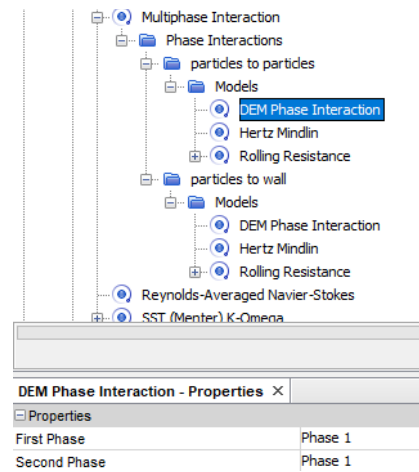
Particle physics:



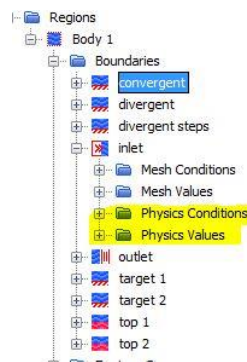


For Injector: Create a probe grid





Step 11: Set proper physics at every region



Step 12: Initialize the solution



Step 13: Run the Simulation



Visualization

Particle Injection

Stepped Nozzle- 500 particles per second

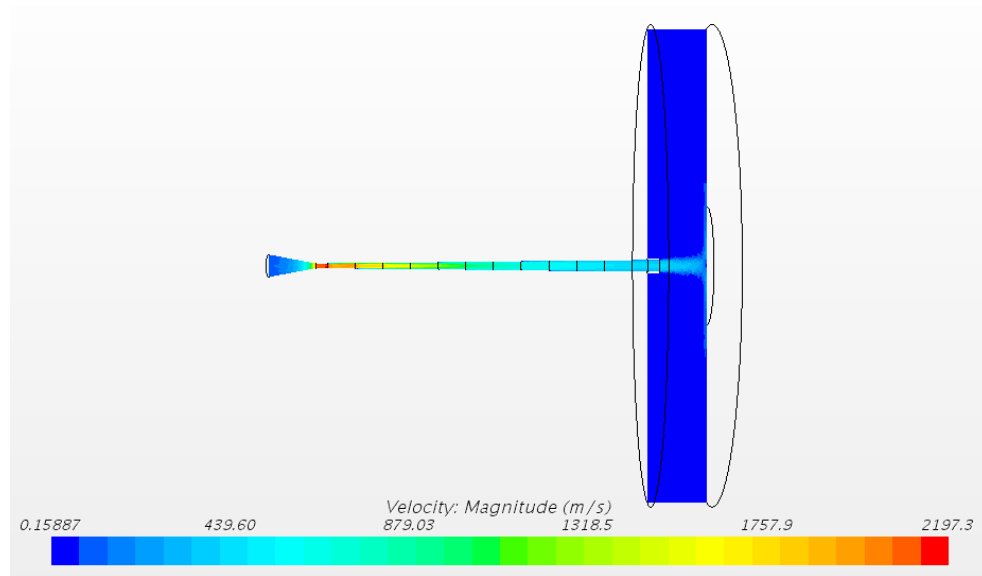


Figure 12: Visualization of Velocity Magnitude in Step Drilled Nozzle

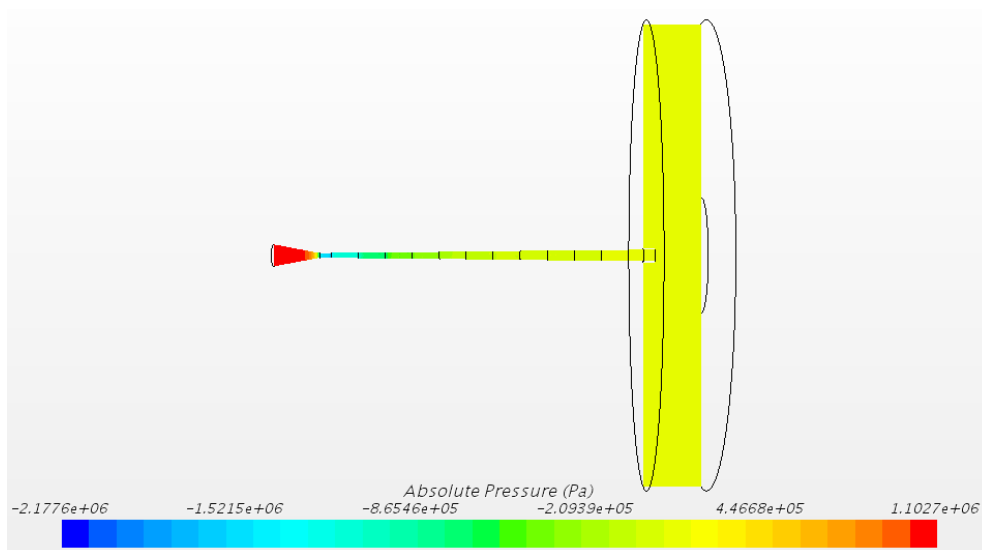


Figure 13: Visualization of Absolute Pressure in Step Drilled Nozzle

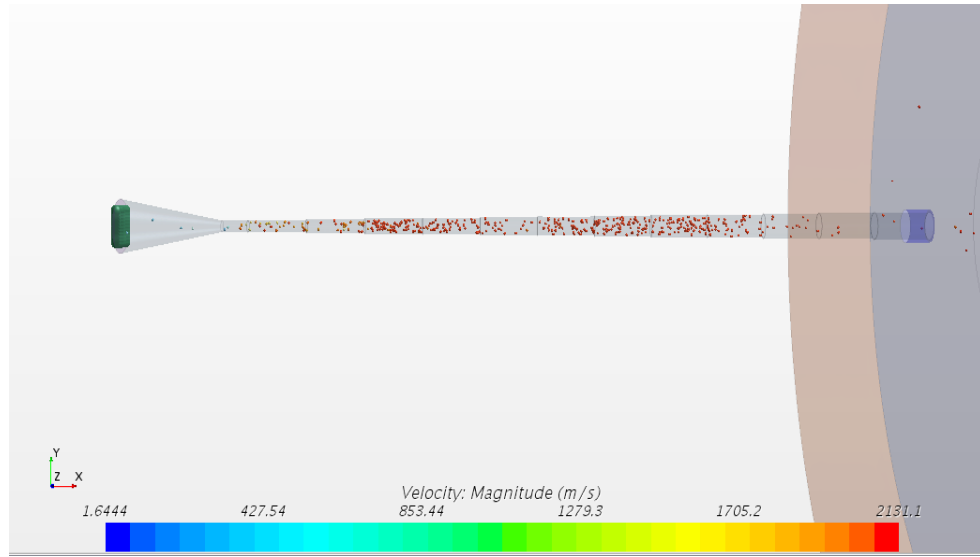


Figure 14: Visualization of 500 particles per second in Step Drilled Nozzle

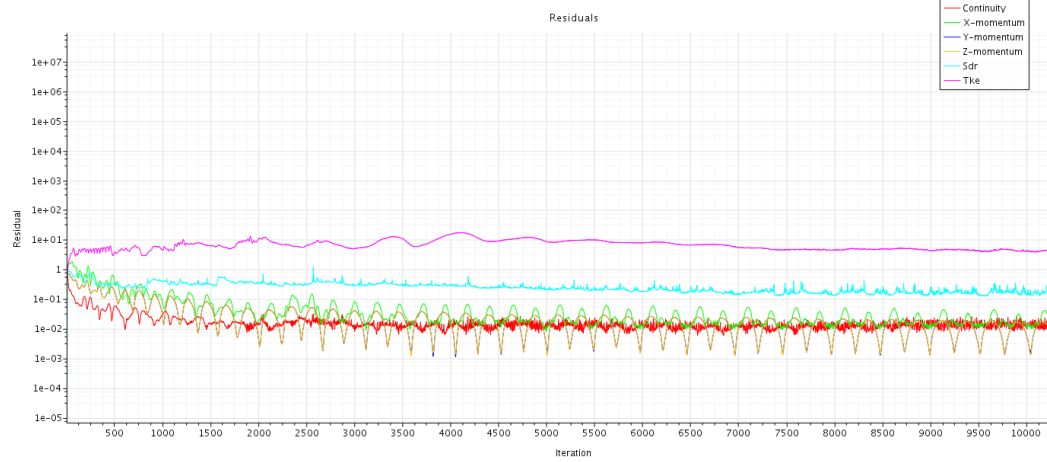


Figure 15: Visualization of residual plot for Step Drilled Nozzle

Stepped Nozzle- 1000 particles per second

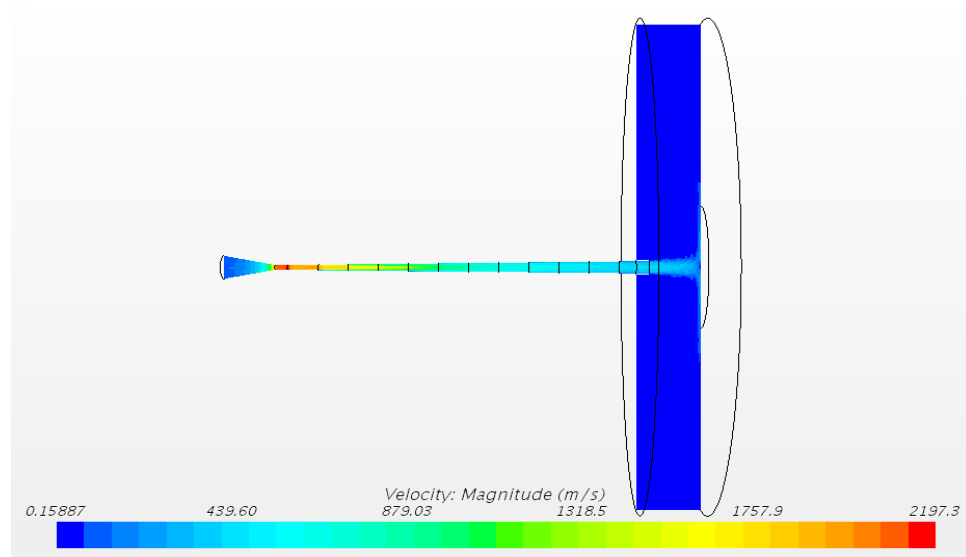


Figure 16: Visualization of Velocity Magnitude in Step Drilled Nozzle

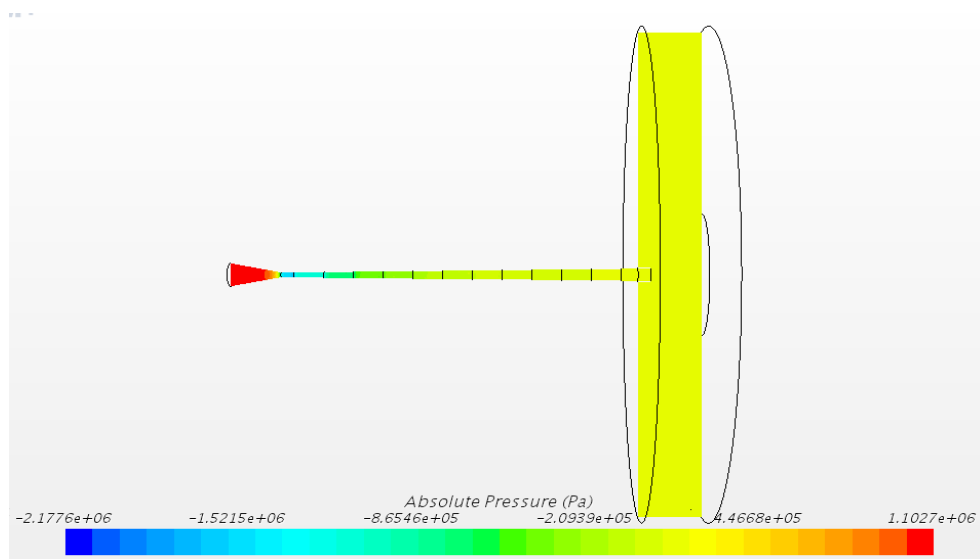


Figure 17: Visualization of Absolute Pressure in Step Drilled Nozzle

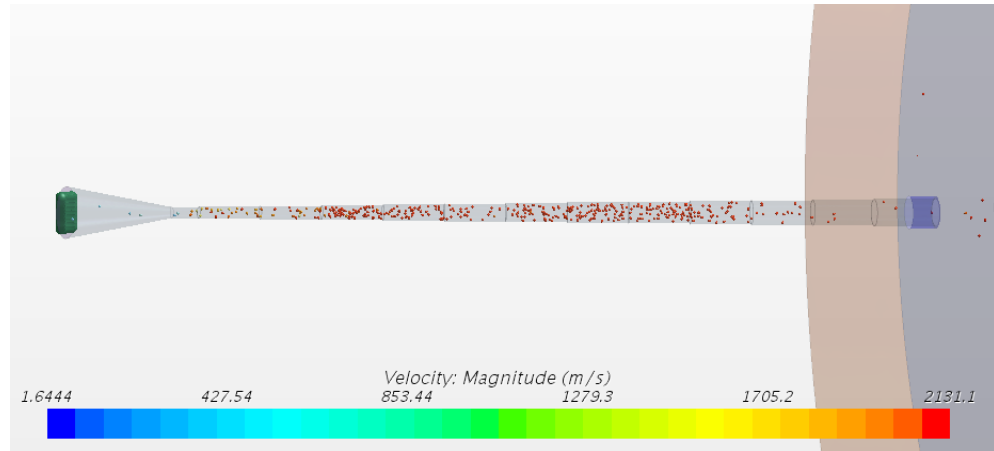


Figure 18: Visualization of 1000 particles per second in Step Drilled Nozzle

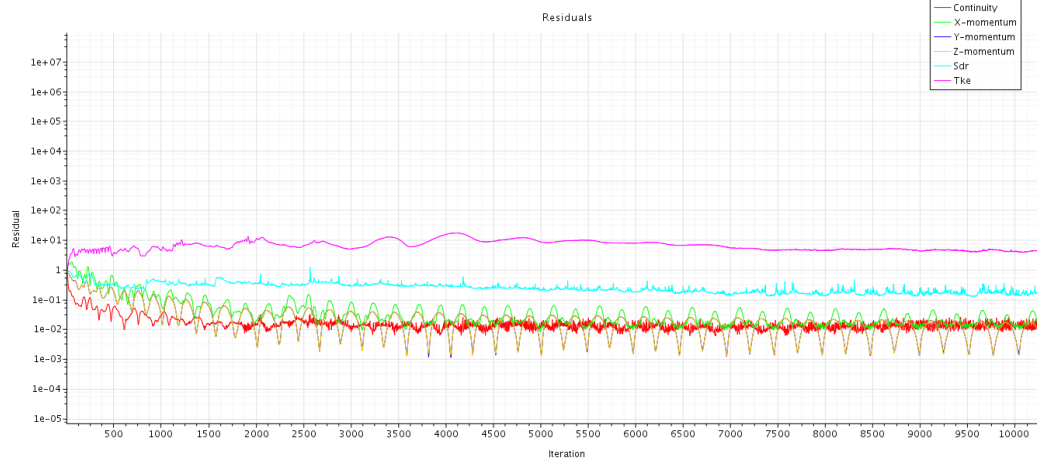


Figure 19: Visualization of residual plot for Step Drilled Nozzle

Stepped Nozzle- 2000 particles per second

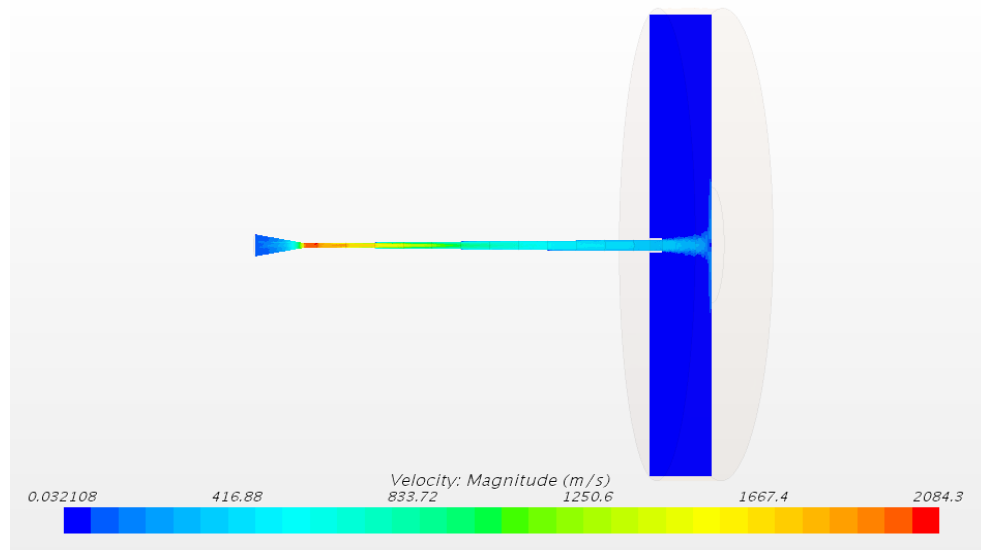


Figure 20: Visualization of Velocity Magnitude in Step Drilled Nozzle

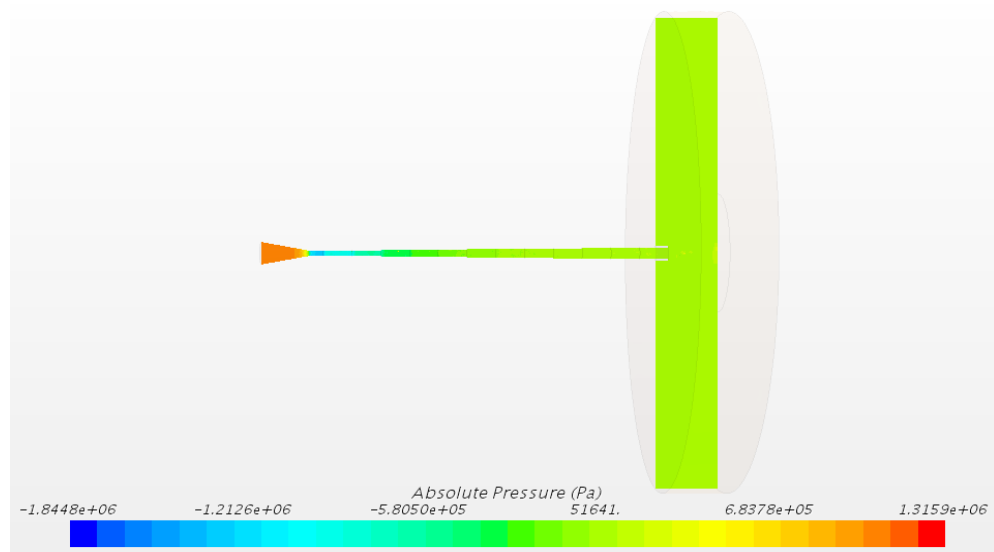


Figure 21: Visualization of Absolute Pressure in Step Drilled Nozzle

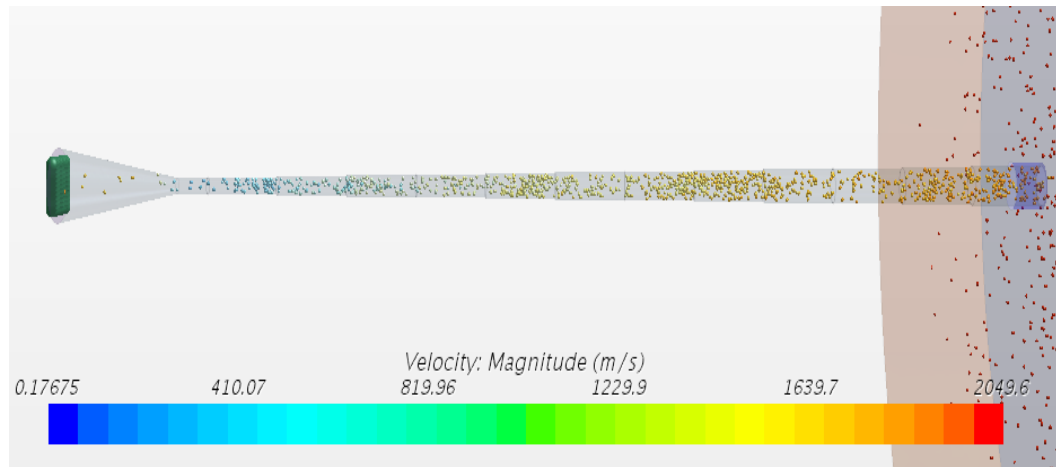


Figure 22: Visualization of 2000 particles per second in Step Drilled Nozzle

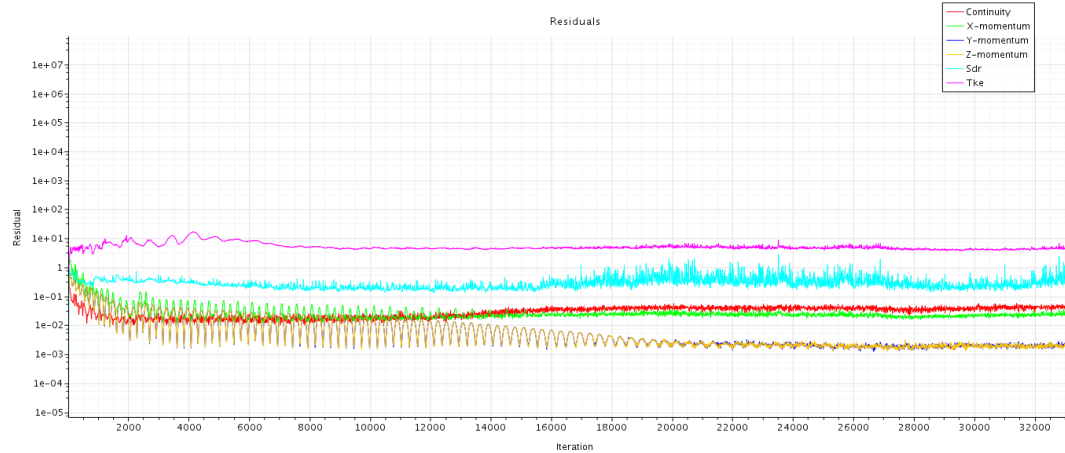


Figure 23: Visualization of residual plot for Step Drilled Nozzle

Carrier gasses with particles Nitrogen - 2000 particles per second

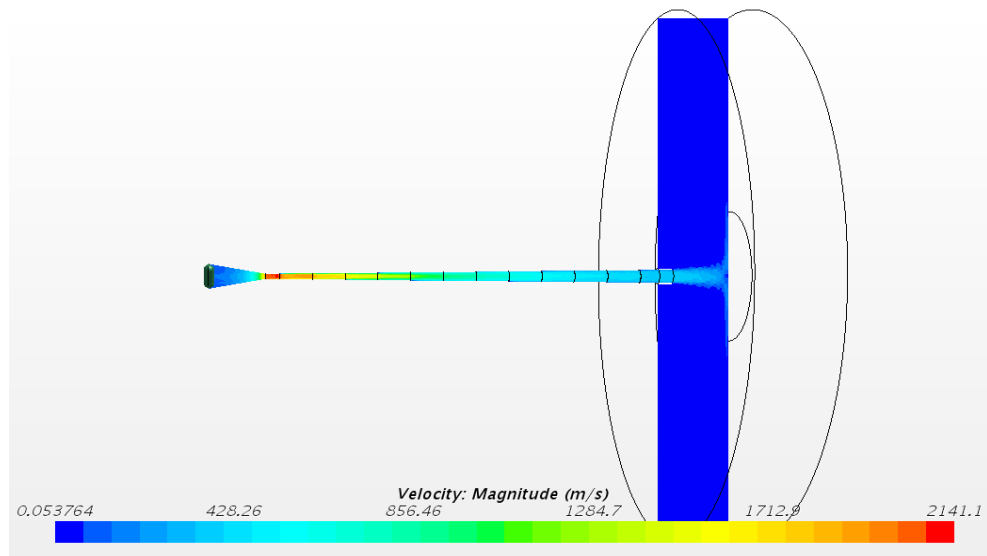


Figure 24: Visualization of Velocity Magnitude in Step Drilled Nozzle with Nitrogen

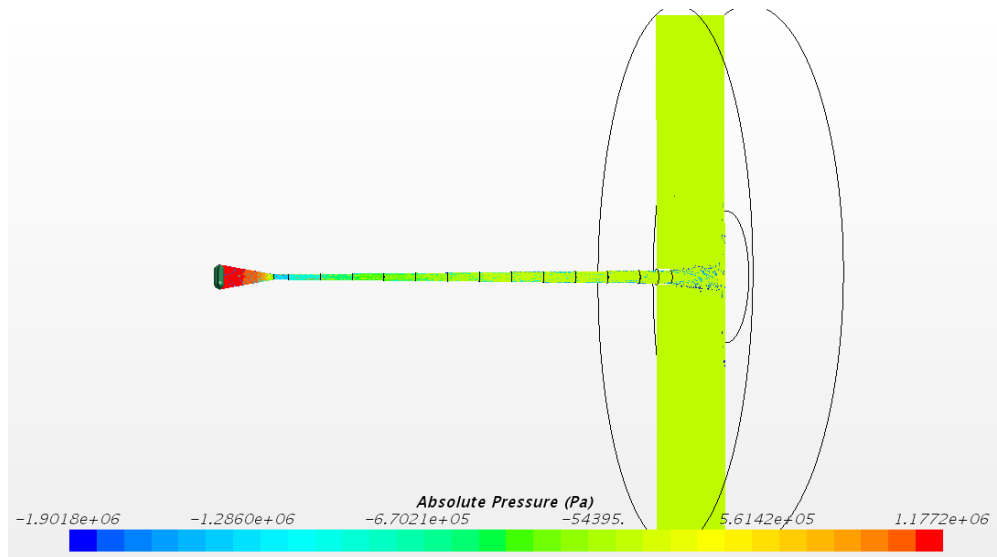


Figure 25: Visualization of Absolute Pressure in Step Drilled Nozzle with Nitrogen

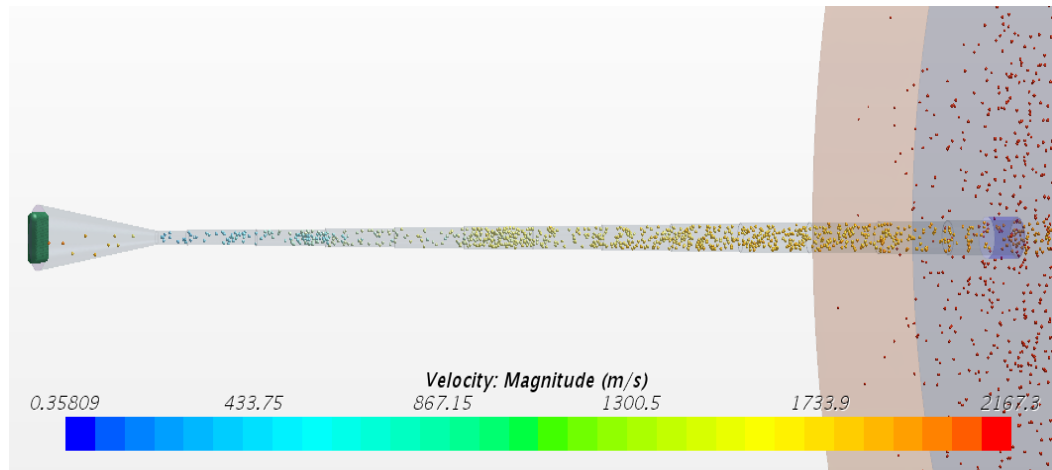


Figure 26: Visualization of 2000 particles per second in Step Drilled Nozzle with Nitrogen

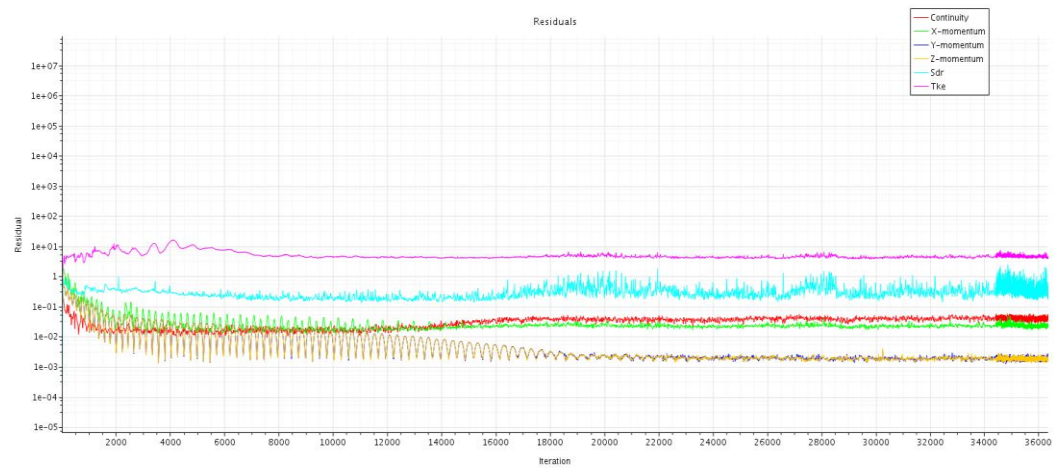


Figure 27: Visualization of residual plot for Step Drilled Nozzle with Nitrogen

Nitrogen - 1000 particles per second

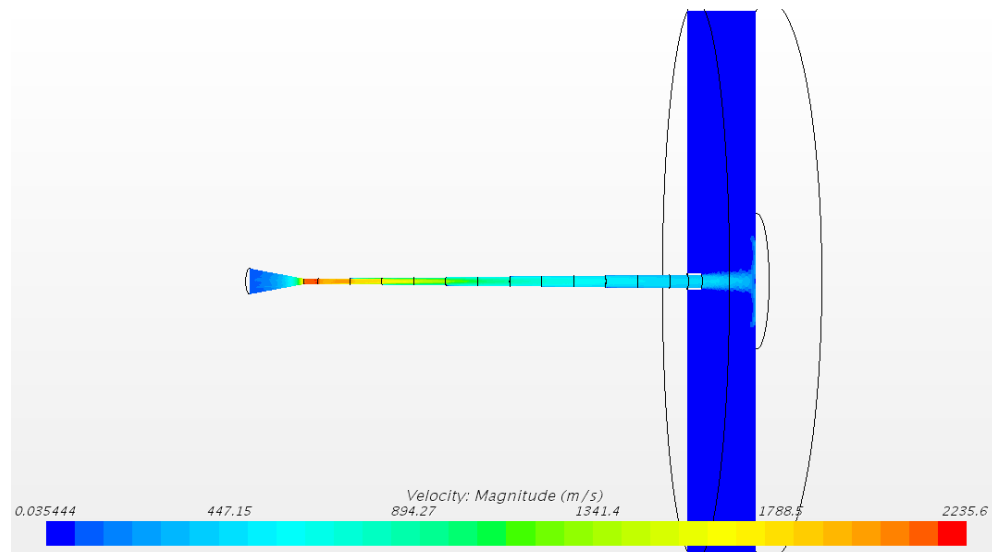


Figure 28: Visualization of Velocity Magnitude in Step Drilled Nozzle with Nitrogen

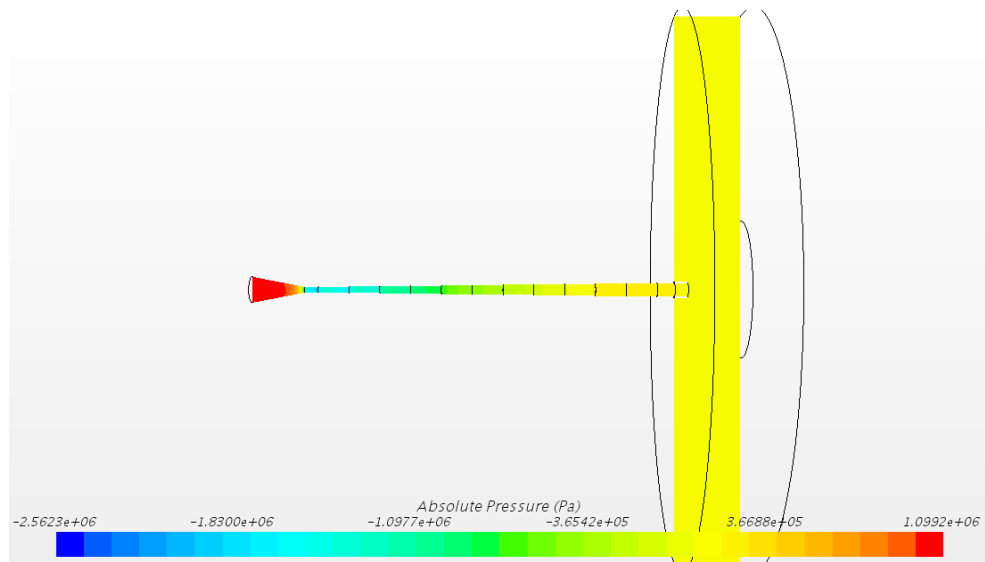


Figure 29: Visualization of Absolute Pressure in Step Drilled Nozzle with Nitrogen

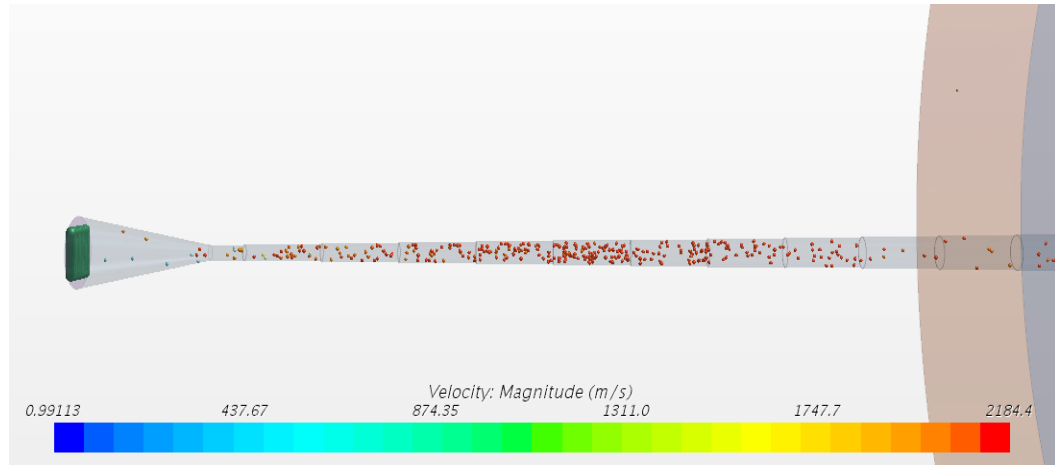


Figure 30: Visualization of 1000 particles per second in Step Drilled Nozzle with Nitrogen



Figure 31: Visualization of residual plot for Step Drilled Nozzle with Nitrogen

Nitrogen - 500 particles per second

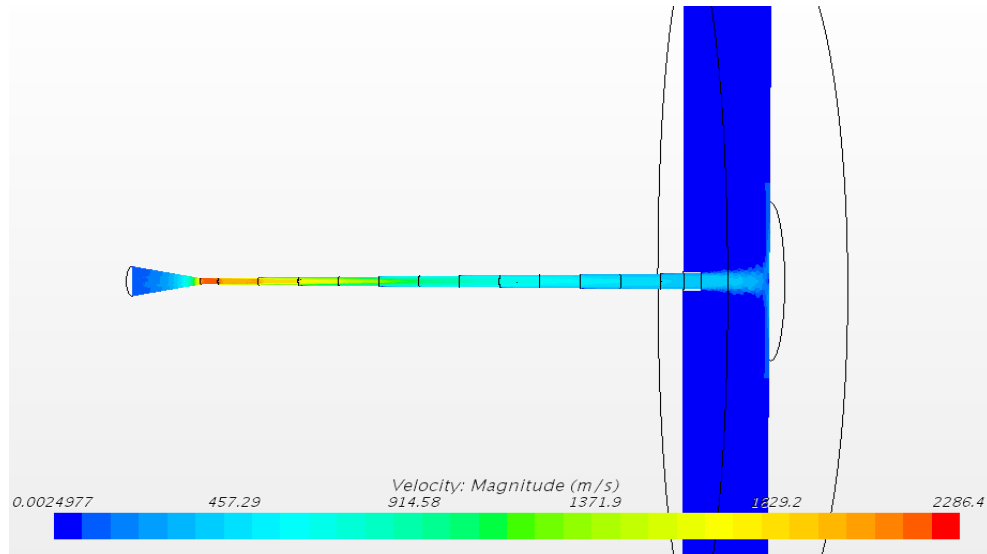


Figure 32: Visualization of Velocity Magnitude in Step Drilled Nozzle with Nitrogen

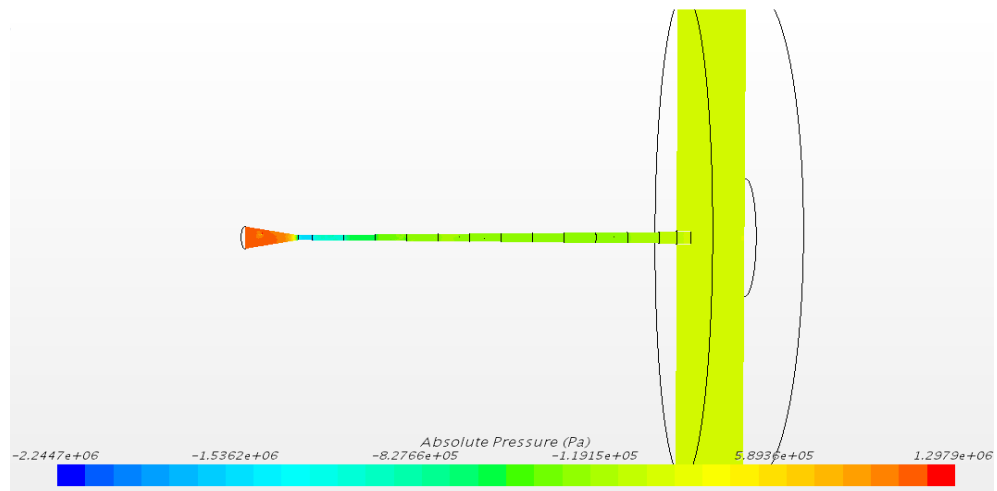


Figure 33: Visualization of Absolute Pressure in Step Drilled Nozzle with Nitrogen

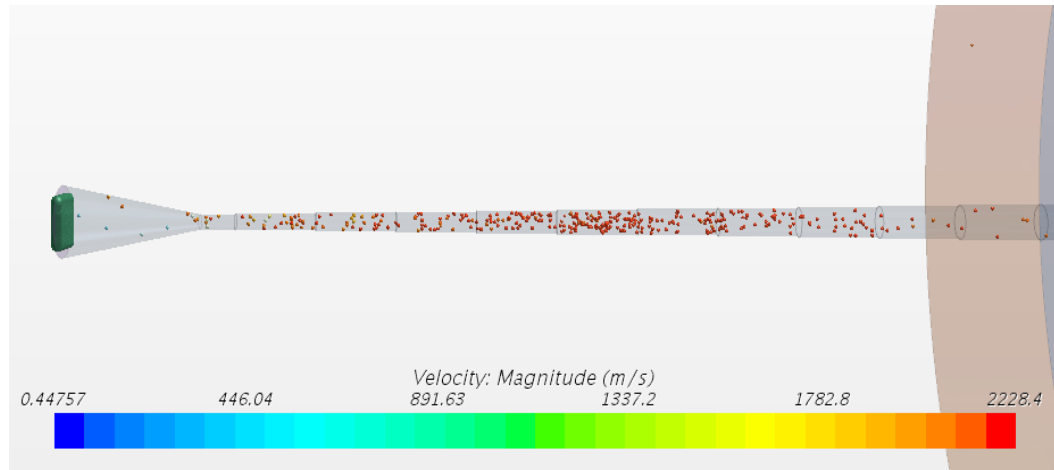


Figure 34: Visualization of 500 particles per second in Step Drilled Nozzle with Nitrogen

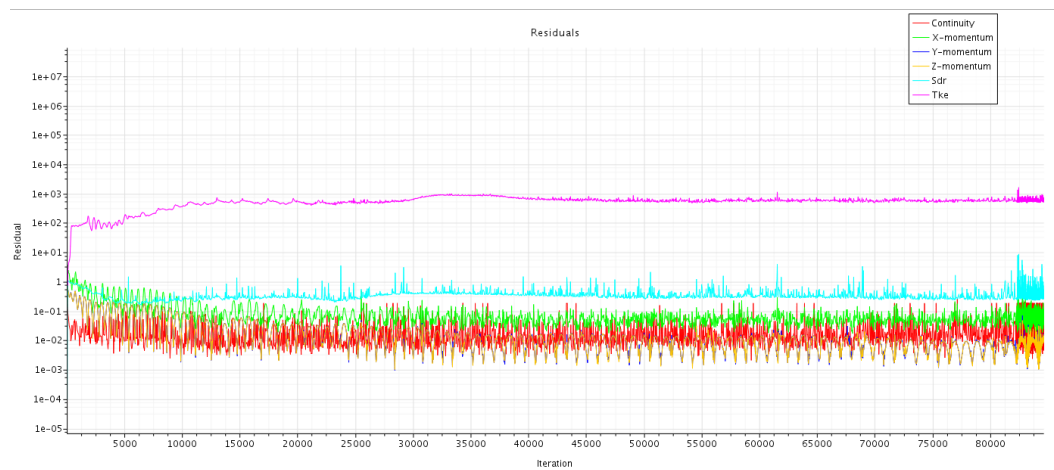


Figure 35: Visualization of residual plot for Step Drilled Nozzle with Nitrogen

Helium - 2000 particles per second

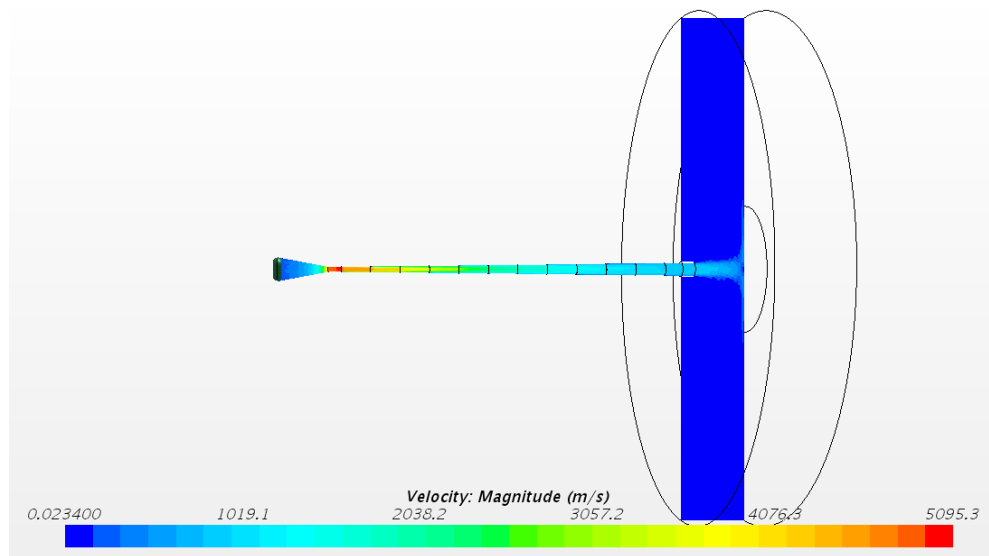


Figure 36: Visualization of Velocity Magnitude in Step Drilled Nozzle with Helium

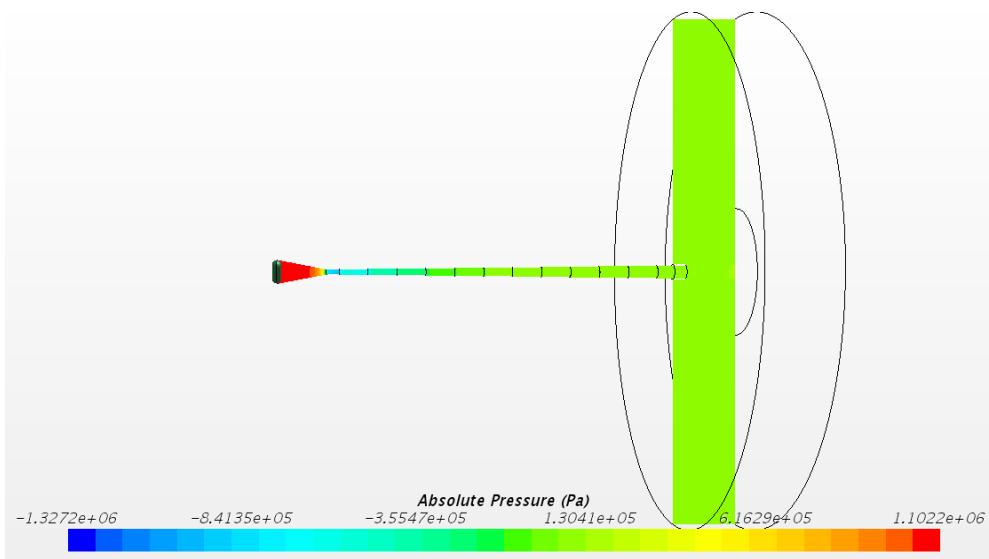


Figure 37: Visualization of Absolute Pressure in Step Drilled Nozzle with Helium

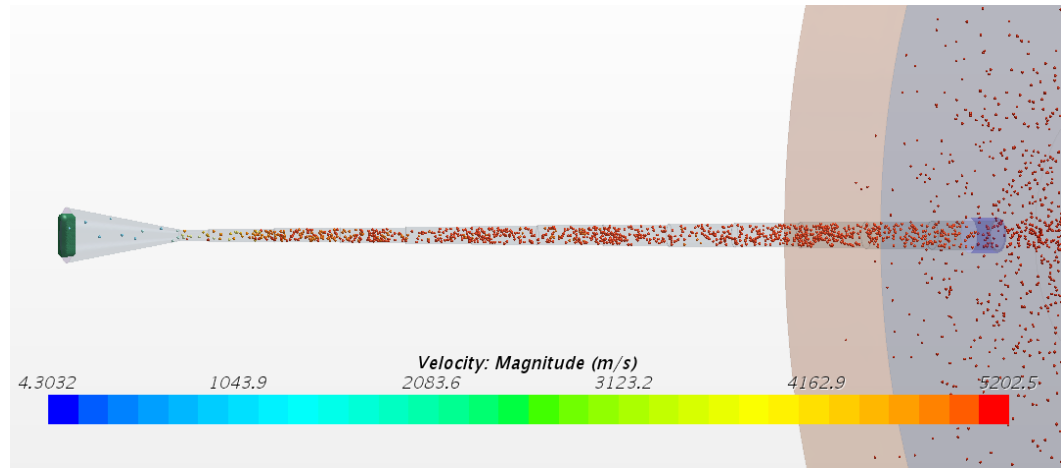


Figure 38: Visualization of 2000 particles per second in Step Drilled Nozzle with Helium

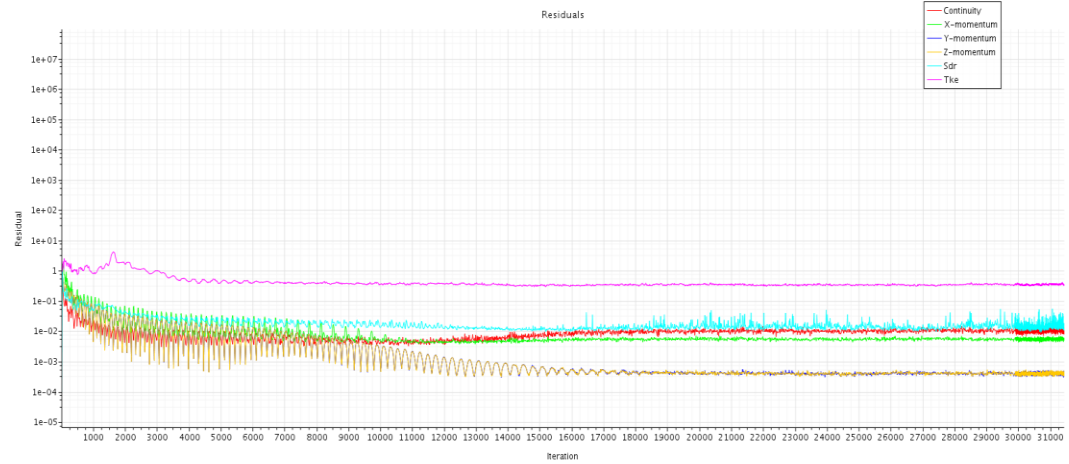


Figure 39: Visualization of residual plot for Step Drilled Nozzle with Helium

Helium - 1000 particles per second

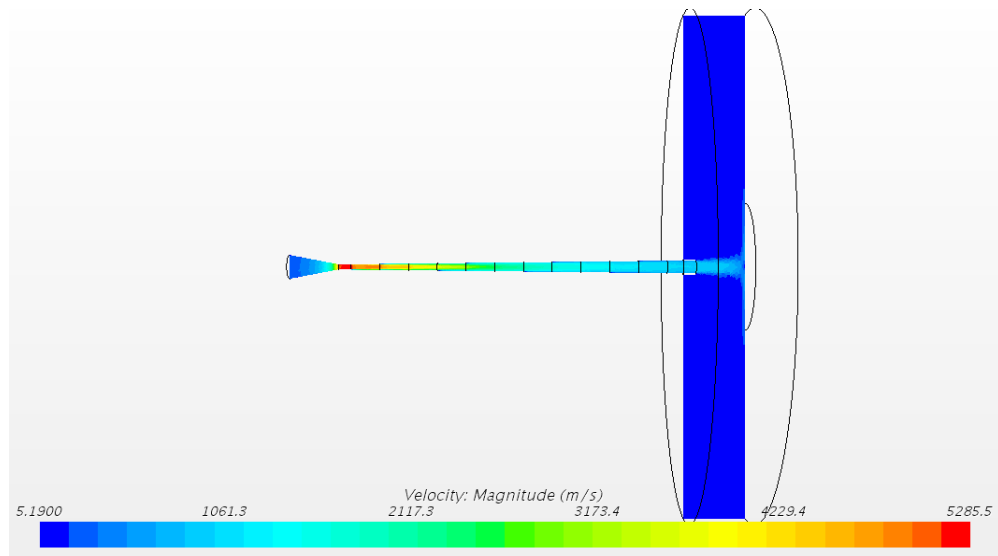


Figure 40: Visualization of Velocity Magnitude in Step Drilled Nozzle with Helium

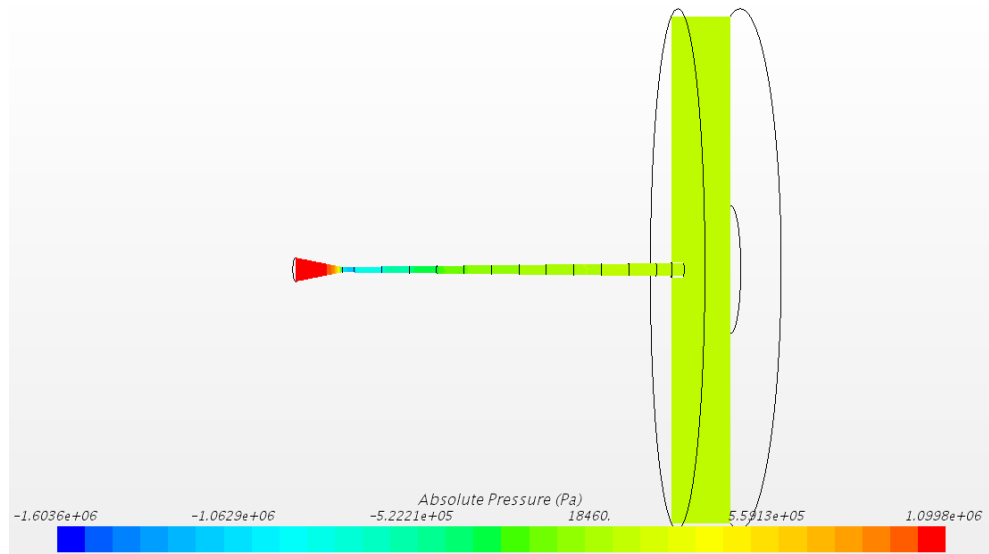


Figure 41: Visualization of Absolute Pressure in Step Drilled Nozzle with Helium

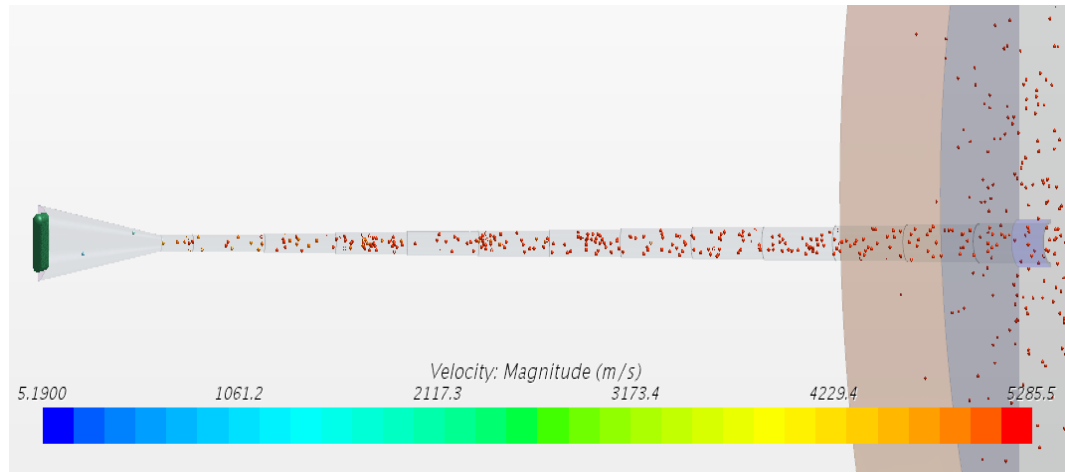


Figure 42: Visualization of 1000 particles per second in Step Drilled Nozzle with Helium



Figure 43: Visualization of residual plot for Step Drilled Nozzle with Helium

Helium - 500 particles per second

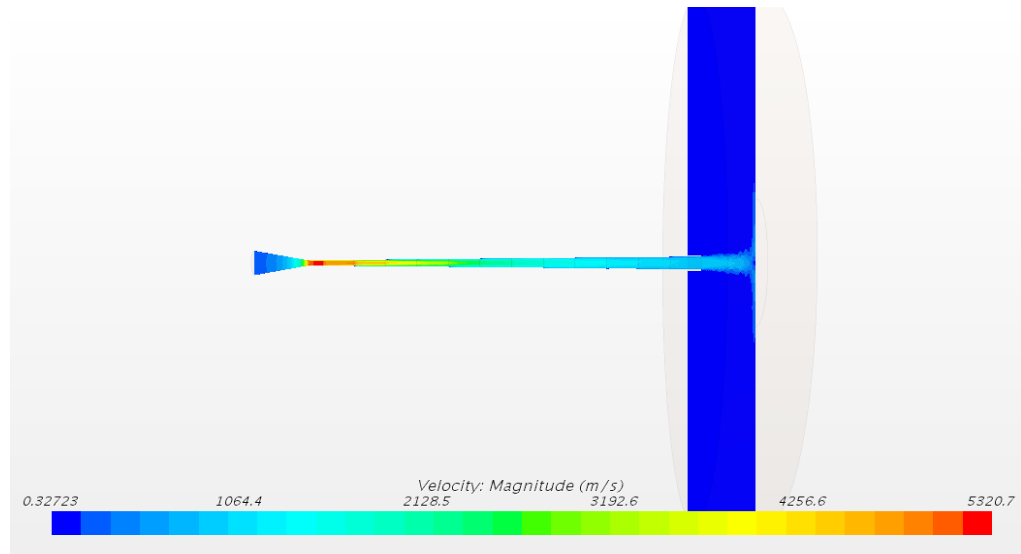


Figure 44: Visualization of Velocity Magnitude in Step Drilled Nozzle with Helium

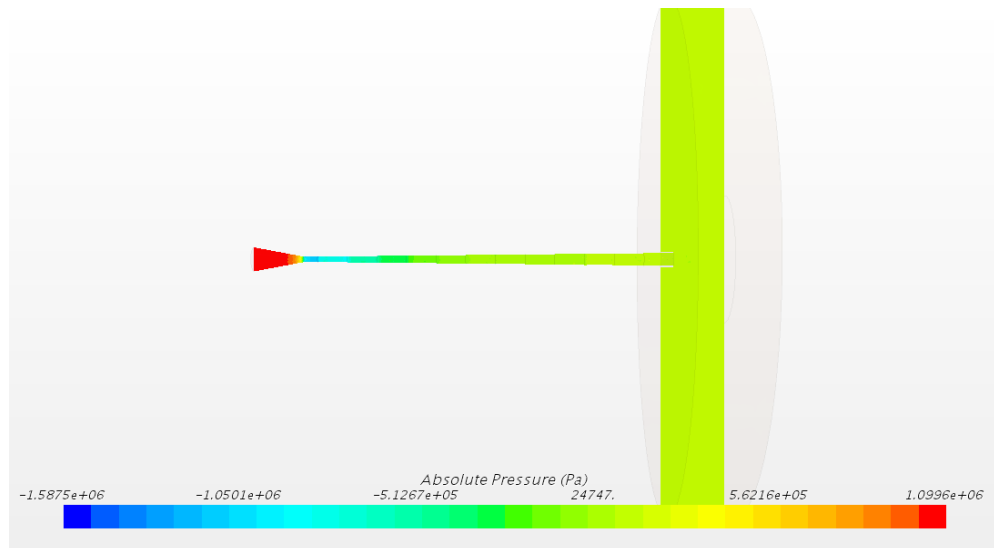


Figure 45: Visualization of Absolute Pressure in Step Drilled Nozzle with Helium

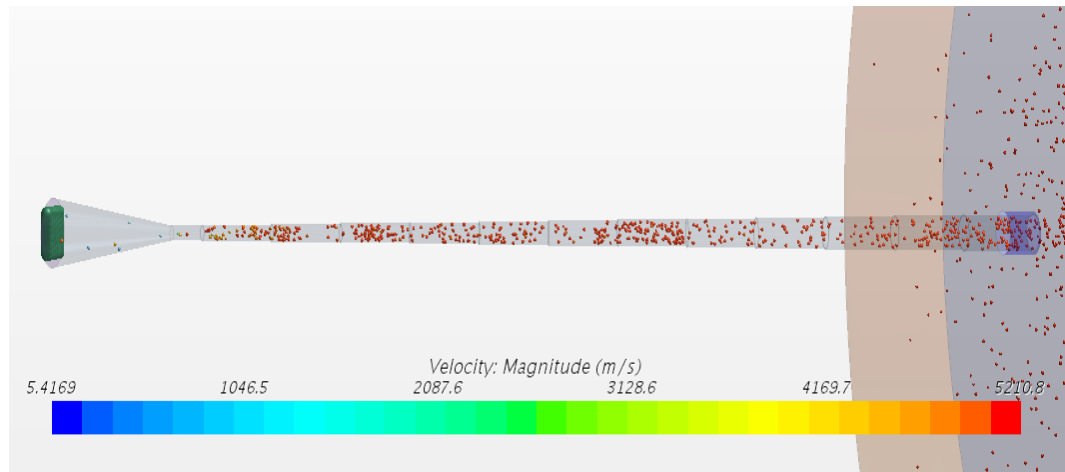


Figure 46: Visualization of 500 particles per second in Step Drilled Nozzle with Helium

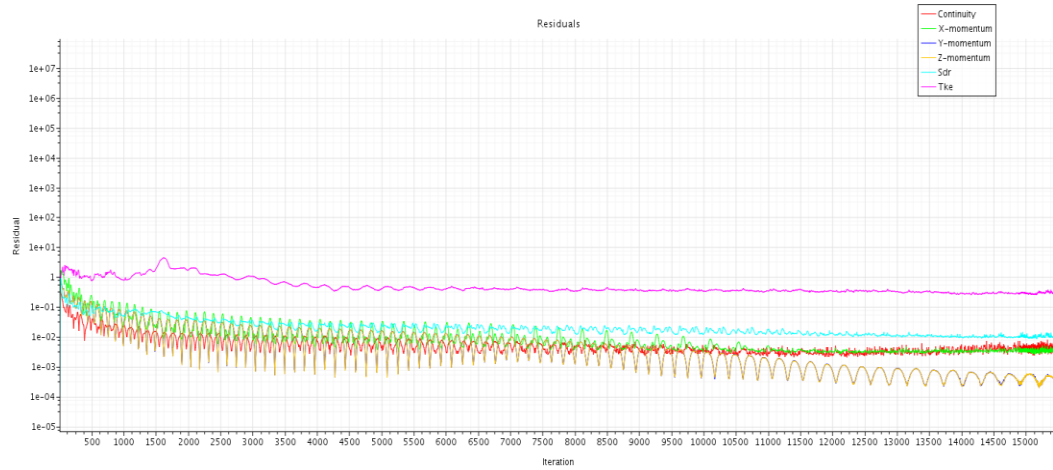


Figure 47: Visualization of residual plot for Step Drilled Nozzle with Helium

Summary of the Results

The procedure needed to create a particle simulation must be followed in the order they are presented to achieve a successful simulation. One of the most important steps is step 6: the meshing control variables, this step is dependent on how intricate the CAD model is and if the model has smaller parts. For smaller detailed parts of the body it will be necessary to apply custom meshing options as shown in step 7. Once the mesh is fine-tuned and all the parts are adequately visualized in the meshing scene, we can proceed to the physics models. For the particle physics, the material of the particles needs to be changed to a desired material, for example, in this study copper particles were used and specified since copper is one of the most commonly used in the literature review studied. Once the particle material has been selected, we must create an injector as shown and define the particle flow rate desired. After all the physics models are chosen and parameters are specified, we move on to the green flag to ensure all the physics are specified correctly if not Star CCM+ will give you an error indicating what is potentially incorrect or incomplete. If Star gives you the green light, you may run the simulations by clicking the running man until a steady state is achieved. This can be determined when the residual plots stabilize.

The visualization of the particles shows us that the particles are affecting the velocity of the flow. As the particles continue to develop through the nozzle, we can observe that the particles increase their velocity and the flow decreases in velocity respectively. This can be attributed to the coupling physics. Various attempts to couple the flow properly with the particles were done in differing simulations. On the visualization of the particles we can see that the behavior of the particles is as expected.

The particles start to accelerate once they reach the throat section of the nozzle and begin reaching a critical velocity between 800 m/s and 1000 m/s at about 34 mm into the diverging section. Similar particle behavior was observed between the 500 particles per second and the 1000 particles per second simulations. Now, for the 2000 particles simulation we can observe that the particles take about 82mm to reach their critical velocity. This behavior is as expected as we have doubled the number of particles flowing through the nozzle with comparison to 1000 particles per second. The particles would take longer to fully develop and reach their critical velocity at this flow rate.

The other concept that was studied in this thesis was how different carrier gasses would affect the flow. The carrier gasses studied were air, nitrogen, and helium. Based on the simulations conducted with air, it was found that the maximum velocity was 2084.3 m/s. For simulations done with nitrogen, it was found that the maximum velocity increased slightly to 2141.1 m/s. The simulations done with helium as the carrier gas found that the maximum velocity increased exponentially to 5095.3 m/s. After observing the simulations with the different gasses, we can conclude that we can reach a critical particle velocity much easier when using helium as the carrier gas. The use of nitrogen with respect to air does not provide a significant increase in velocity, that was found to be only 2%. In helium, we see more than twice as much potential capabilities at 59% when compared to air and 57% when compared to nitrogen. In real-life application, helium would be a better carrier gas because it can carry a wider variety of materials more effectively than nitrogen or air respectively. Another parameter that can be considered when working with helium is that less pre-heating is required and the system can operate at a lower pressure to achieve similar results to air.

Validation

Validation is performed by comparing the results of Muhammad Faizan Ur Rab's simulation [25] to the results obtained by a conical nozzle simulation with the same parameters used in this study. Figure 48 shows the computed velocity profile concerning the nozzle axis for cold spray supersonic jet at 800C and 3 MPa. Figure 49 shows the calculated velocity profile concerning the nozzle axis for cold spray supersonic jet at 250 °C and 3.2 MPa. As it can be seen from the velocity profiles of the validation case and the simulation, the velocity along the axis on both nozzles exhibit striking similarity in the trend. Both the nozzles witness significant acceleration in velocity when the gas enters the diverging section, a gradual increase in the velocity until the gas exits the nozzle, negative peak during the travel in the stand-off distance and comes down to zero when the gas impacts the surface of the substrate. Since the process variables vary in both cases, the velocity magnitude varies but not the trend observed. Table 4 shows the differences in the process variables. Since there are not many research articles published on a step drilled nozzle used for cold spray, further investigation regarding experimentation and modeling will be required in future work for more exact comparisons and validation. Therefore, it is sensible to conclude that the simulation results obtained for the this study are validated.

	Current Study	Validation Case
Gas Inlet Pressure, MPa	3.2	3
Gas Inlet Temperature, C	250	800
Gas Type	Air	Nitrogen
Nozzle Throat Diameter, mm	2	2.7
Stand Off Distance, mm	20	35
Convergent Section Length, mm	20	51.2
Divergent Section Length, mm	145	70.3
Divergent Section Profile	Stepdrilled	Conical

Table 4: Summary of Process Variables used in validation case and current case

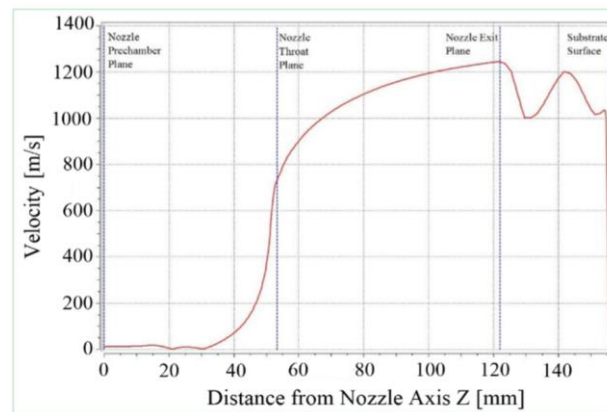


Figure 48: Calculated Velocity profile concerning the nozzle axis for cold spray supersonic jet at 800 C and 3 MPa [Validation Case]

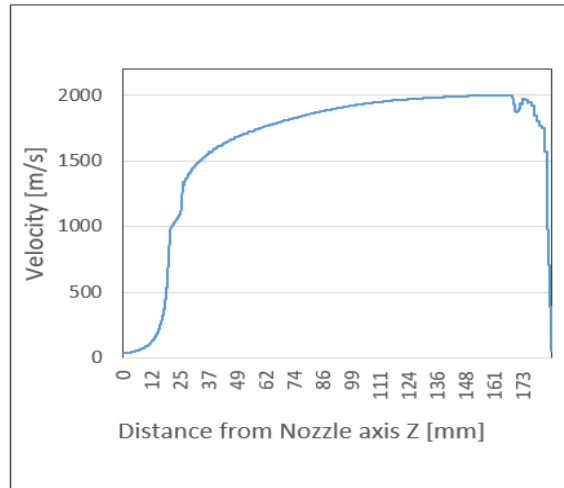


Figure 49: Computed velocity profile in the nozzle axis for cold spray supersonic nozzle jet 250 C and 3.2 MPa [current study]

Research Contribution

This research study contributes to the numerical analysis performed on the step drill nozzle. In this study, the behaviour of the particles inside the nozzle are studied while certain parameters were changed. The same parameters were tested with differing carrier gasses to study how they would affect the particle behaviour throughout the nozzle. This study helps us understand how particles behave and how to properly create a particle simulation in a cold spray nozzle.

This study contributes to research by establishing the proper procedures to create a super sonic jet particle cold spray simulation. The physics that are used for this study have been interpreted from past research done in the subject, such as the literature review and by applying trial and error methods to simulations ran. Proper visualization of particles has been achieved in a scalar form, which is easily understandable. Particle behaviour can be analysed for cold spray nozzles with similar parameters. The carrier gas study demonstrates how different carrier gasses provide performances in velocity.

CHAPTER 5: CONCLUSION AND FUTURE WORK

The conclusion of the thesis in this section provides with some suggestions for future work in this area. The proper procedure was established and broken down to make particle simulations easier to create and study. The results obtained are summarized as follows:

- The step by step procedure was created to establish a more streamlined method of creating particle simulations on Star CCM+
- The careful observation and analysis of the behavior of the particles was done to understand how the particles flowed throughout the different sections of the nozzle.
- The carrier gas study demonstrates that helium would be a better carrier gas than air or nitrogen, due to its performance increase of 59% and 57% respectively.

This thesis has been mainly focused on analyzing the behavior of particles being injected into nozzles and the analysis of different carrier gases, leaving the study of particle interaction in the nozzle outside the scope of the thesis. Future work for this project include:

- Introducing coupling interactions between the particles and the nozzle wall
- Performing Large Eddy simulations for more detailed analysis
- Design De-Laval nozzles using the equations mentioned in the current study
- Performing research study on the shock formation inside the nozzle
- Using different nozzles with particle simulations

REFERENCES

1. "Bonding mechanism in cold gas spraying." *Acta Materialia* 51(15): 4379-4394.
2. S.H. Thurston, Method of Impacting One Metal Upon Another, US706701, year of priority (issued): 1900 (1902)
3. C.F. Rocheville, Device for Treating the Surface of a Workpiece, US3100724, year of priority (issued): 1958 (1963)
4. Papyrin, V. Kosarev, K.V. Klinkov, A. Alkhimov, and V.M.Fomin, Cold Spray Technology. Elsevier, Oxford, 2006
5. A.I.Kashirin, O.F. Klyuev, and .V. Buzdygar: 'Apparatus for gas-dynamic coating,' US Patent 6402050, 2002.
6. "Cold spray coating: review of material systems and future perspectives." *Surface Engineering* 30(6): 369-395.
7. "Cold spraying: From process fundamentals towards advanced applications." *Surface & Coating Technology*, 2014
8. T. H. Van Steenkiste, J. R. Smith, D. W. Gorkiewicz, A. A. Elmoursi, B. A. Gillispie, and N. B. Patel: 'Method of maintaining a non-obstructed interior opening in kinetic spray nozzles,' US Patent 6896933, 2005.
9. A.S.M. Ang, N. Sanpo, M.L. Sesso, S.Y. Kim, C.C. Berndt, J. *Thermal Spray Technology* 22 (7) (2013) 1170-1183
10. T. Stoltenhoff, H. Kreye, H.J. Richter "An analysis of cold spray process and its coatings." ASM International

11. A. Arabgol, H. Assadi, T. Schmidt, F. Gartner, and T. Klassen, Analysis of Thermal History and Residual Stress in Cold-Sprayed Coatings, *J. Thermal Spray Technology*, Vol 23 (No. 1-2), 2014, p 84-90]
12. Shuo Yin, Xiao-fang Wang, Wen-ya Li, "Computational analysis of the effect of nozzle cross-section shape on gas flow and particle acceleration in cold spraying." *Surface & Coatings Technology*
13. Masahiro Fukumoto, Hiroki Terada, Masahiro Mashiko, Kazunori Sato, Motohiro Yamada and Eiji Yamaguchi "Deposition of Copper Fine particle by the cold spray process."
14. "Optimal design of a cold spray nozzle by numerical analysis of particle velocity and experimental validation with 316L stainless steel powder." *Materials & Design* 28(7): 2129-2137.
15. "Optimal design of a convergent-barrel cold spray nozzle by numerical method." *Applied Surface Science* 253(2): 708-713.
16. Zheng-Dong, Zhang Guo-qing, Zhou, Zhang Yong, Xu Wen-Yong, "Simulation of Gas Flow Field in Laval Nozzle and Straight Nozzle for Powder Metallurgy and Spray Forming," *Journal of Iron and Steel Research*, 2008
17. "Numerical investigations on the effect of total pressure and nozzle divergent length on the flow character and particle impact velocity in cold spraying." *Surface and Coatings Technology* 232: 290-297.
18. "Design and optimization of rectangular cold spray nozzle: Radial injection angle, expansion ratio and traverse speed." *Surface and Coatings Technology* 316: 246-254.

19. "An analysis of the particulate flow in cold spray nozzles." *Mechanical Sciences* 6(2): 127-136.
20. "Significant influence of carrier gas temperature during the cold spray process." *Surface Engineering* 30(6): 443-450.
21. "Numerical Simulation of the Cold Gas-Dynamic Spray Process." *Journal of Thermal Spray Technology* 15(4): 518-523.
22. R. Lupoi and O'Neill, "Powder stream characteristics in cold spray nozzles." *Surface & Coatings Technology* 206 (2011)
23. "Numerical study on the effect of nozzle dimension on particle distribution in cold spraying." *Surface and Coatings Technology* 220: 107-111.
24. M Grujicic, W S DeRosset, D Helfritch "Flow analysis and nozzle-shape optimization for the cold-gas dynamic-spray process."
25. Muhammad Faizan Ur Rab, Saden Zahiri, Syed H. Masood, Mahnaz Jahedi and Romesh Nagarajah "Development of 3D Multicomponent Model for Cold Spray Process Using Nitrogen and Air."
26. "Current design and performance of cold spray nozzles: experimental and numerical observations on deposition efficiency and particle velocity." *Surface Engineering* 30(5): 316-322.
27. Chang-Jiu Li, Wen-Ya Li, Yu-Yue Wang, Guan-Jun Yang, H. Fukanuma "A theoretical model for prediction of deposition efficiency in cold spraying."
28. Li, W. Y., Zhang, D. D., Huang, C. J., Yin, S., Yu, M., Wang, F. F., & Liao, H. L. (2014). Modelling of impact behaviour of cold spray particles: review. *Surface Engineering*, 30(5), 299–308. <https://doi.org/10.1179/1743294414Y.0000000268>

29. Villafuerte, J. (2010). Recent trends in cold spray technology: looking at the future. *Surface Engineering*, 26(6), 393–394.
<https://doi.org/10.1179/026708410X12687356948715>
30. Karimi, M., Fartaj, A., Rankin, G., Vanderzwet, D., Birtch, W., & Villafuerte, J. (2006). Numerical simulation of the cold gas dynamic spray process. *Proceedings of the International Thermal Spray Conference*, 15(December), 518–523.
<https://doi.org/10.1361/105996306X146866>
31. Schmidt, T., Assadi, H., Gärtner, F., Richter, H., Stoltenhoff, T., Kreye, H., & Klassen, T. (2009). From particle acceleration to impact and bonding in cold spraying. *Journal of Thermal Spray Technology*, 18(5–6), 794–808.
<https://doi.org/10.1007/s11666-009-9357-7>
32. Grujicic, M., Tong, C., DeRosset, W. S., & Helfrich, D. (2003). Flow analysis and nozzle-shape optimization for the cold-gas dynamic-spray process. *Proceedings of the Institution of Mechanical Engineers, Part B: Journal of Engineering Manufacture*, 217(11), 1603–1613.
<https://doi.org/10.1243/095440503771909980>
33. Suo, X. K., Liu, T. K., Li, W. Y., Suo, Q. L., Planche, M. P., & Liao, H. L. (2013). Numerical study on the effect of nozzle dimension on particle distribution in cold spraying. *Surface and Coatings Technology*, 220, 107–111.
<https://doi.org/10.1016/j.surfcoat.2012.09.029>
34. Karaoglanli, A. C., Turk, A., & Ozdemir, I. (2016). Effect of sintering on mechanical properties of cold sprayed thermal barrier coatings. *Surface Engineering*, 32(9), 686–690. <https://doi.org/10.1080/02670844.2016.1182959>